

# Open bottom mesons in hot asymmetric hadronic medium

Divakar Pathak<sup>\*</sup> and Amruta Mishra<sup>†</sup>

*Department of Physics, Indian Institute of Technology,  
Delhi, Hauz Khas, New Delhi – 110 016, India*

## Abstract

The in-medium masses and optical potentials of  $B$  and  $\bar{B}$  mesons are studied in an isospin asymmetric, strange, hot and dense hadronic environment using a chiral effective model. The chiral  $SU(3)$  model originally designed for the light quark sector, is generalized to include the heavy quark sector ( $c$  and  $b$ ) to derive the interactions of the  $B$  and  $\bar{B}$  mesons with the light hadrons. Due to large mass of bottom quark, we use only the empirical form of these interactions for the desired purpose, while treating the bottom degrees of freedom to be frozen in the medium. Hence, all medium effects are due to the in-medium interaction of the light quark content of these open-bottom mesons. Both  $B$  and  $\bar{B}$  mesons are found to experience net attractive interactions in the medium, leading to lowering of their masses in the medium. The mass degeneracy of particles and antiparticles,  $(B^+, B^-)$  as well as  $(B^0, \bar{B}^0)$ , is observed to be broken in the medium, due to equal and opposite contributions from a vectorial Weinberg-Tomozawa interaction term. Addition of hyperons to the medium lowers further the in-medium mass for each of these four mesons, while a non-zero isospin asymmetry is observed to break the approximate mass degeneracy of each pair of isospin doublets. These medium effects are found to be strongly density dependent, and bear a considerably weaker temperature dependence. The results obtained in the present investigation are compared to predictions from the quark-meson coupling model, heavy meson effective theory, and the QCD Sum Rule approach.

PACS numbers: 12.39.Fe; 12.38.Lg; 11.30.Rd; 21.65.Jk; 21.65.Cd

---

<sup>\*</sup> [dpdlin@gmail.com](mailto:dpdlin@gmail.com)

<sup>†</sup> [amruta@physics.iitd.ac.in](mailto:amruta@physics.iitd.ac.in)

## I. INTRODUCTION

It is widely recognized that the properties of hadrons in the medium are different from their behavior in vacuum [1–4]. The low-energy dynamics of QCD (i.e. of the hadronic phase) is governed principally by chiral symmetry, whose spontaneous breaking leads to a non-vanishing scalar condensate in vacuum. The properties of the hadrons containing light quark(s) depend on the light quark condensate and are modified in the medium in accord with it [1]. While addressing all these questions of hadronic in-medium behavior, one is essentially in the non-perturbative regime of QCD. In this regime, the perturbative techniques no longer are applicable and there exist diverse techniques to study the medium modifications of the hadrons, which can be broadly grouped into: the coupled channel approach [5–8], QCD sum rules [9–12], quark-meson coupling model [13–15], relativistic mean field approaches based on the Walecka model [16] and its subsequent extensions, and, the method of chiral-invariant Lagrangians. This multitude of approaches provides the additional advantage that while questions of validity of theoretical approaches are conclusively settled only by experimentation, in the temporary absence of experimentation, a comparison between two independent well-founded approaches is still a healthy way of ascertaining whether or not one is on the right track. These medium effects have been predicted to have several important consequences, which also reflects the potential significance of this problem. These range from antikaon condensation [17], sub-threshold production of particles, overall enhancement in dilepton production [18–20], extra decay channels and consequent suppression in the yield of the parent particle (e.g.  $J/\Psi$  suppression [21], for which this is a possible mechanism), unequal particle ratios for isospin pairs in heavy ion collision experiments [22], as well as production asymmetry [23] for antiparticles.

One approach that has been vigorously pursued in the past few years is to treat these medium effects from the point of view of a phenomenological, effective, hadronic Lagrangian based on the QCD symmetries (in particular, the chiral symmetry) and symmetry-breaking patterns [24, 25]. While this was originally devised as a further step in the evolution of this effective Lagrangian approach, which explicitly accounted for these features while these were not a part of the earlier hadrodynamical (Walecka-type) models, this has grown into an extremely productive method which has been fruitfully applied to understand the behavior of matter under extreme conditions of density and temperature. In its original incarnation,

this model was used to successfully describe nuclear matter, finite nuclei, neutron stars and hypernuclei [25]. Subsequently, this was used to understand the in-medium behavior of vector mesons [26, 27], and more extensively, that of kaons and antikaons [28–32], which is natural, given the fact that this model was specifically tailored for the chiral  $SU(3)$  situation. Of late, this approach has been extended to the charm sector in pseudoscalar mesons as well, by generalizing this effective  $SU(3)_L \times SU(3)_R$  model to  $SU(4)$ , and applied to study the in-medium behavior of  $D$  mesons [33–36]. However, since  $SU(4)$  symmetry is badly broken owing to the large mass of the charm quark, these analyses only used this  $SU(4)$  symmetry to derive the empirical form of the interactions, while the charm degrees of freedom were treated as frozen in the medium. Tacitly, therefore, each of these studies treats a  $D$  meson as a heavy-light system of quarks and antiquarks, with the dynamics of the heavy quark frozen. Such a system gets modified in a hadronic medium due to the interactions of the light  $u$  and  $d$  quarks (and anti-quarks) of the open charm meson with the particles constituting the medium, and not because of the heavy quark content. However, from a physical perspective, if the heavy quark is to be treated as frozen, a *light antiquark-bottom* pseudo-scalar meson (e.g.  $\bar{u}b$ ) is similar to a *light antiquark-charm* pseudo-scalar meson (e.g.  $\bar{u}c$ ). In the present investigation, we generalize the chiral effective approach to the bottom sector, and derive the interactions of the  $B$  and  $\bar{B}$  mesons with the light hadrons to determine the in-medium behavior of these *light quark-bottom* meson systems. On the other hand, the heavy quarkonium systems, e.g., charmonium and bottomonium states, due to the absence of any light quark constituents, are modified in the medium due to their interactions with the gluon condensates [36–38]. A study of the mass modification of the charmonium system in the medium arising from the medium modifications of the gluon condensate has been recently generalized to study the bottomonium states in the medium [39].

The topic of the properties of the  $B(\bar{B})$  mesons can also be important in the study of  $B$  meson diffusion, drag and propagation in a hot and/or dense hadronic matter. Heavy flavored mesons are considered to be valuable probes for analyzing the behavior of matter in hot and dense medium, in both the quark-gluon plasma and hadronic phase [40]. This is because they carry a heavy (charm or bottom) quark which has a special significance as regards the experimental characterization of matter formed in a high energy collision. Based on explicit solutions from a Langevin model formulated to study the questions of transport and thermalization of heavy quarks in a quark-gluon plasma [41], it has been reasoned that

the thermal relaxation time for the heavy quarks is significantly larger than that of lighter quarks, due to which these heavy quarks are likely not to reach an equilibrium with their ambience, and hence, (upon subsequent hadronization) still retain information about the initial stages of the heavy ion collision, when these were produced [42]. Thus, analyzing these heavy flavored mesons is an indirect and efficient way of finding out about the early stages of these collisions. This realization has led to a flurry of recent activity [40, 42–45], studying both, the utility of open-bottom mesons as a probe, as well as their transport properties in a hadronic medium. Especially, Refs. [40, 43] establish that not just that the open-bottom mesons do not thermalize at the the kind of energies one encounters at LHC and RHIC,  $B$  mesons are more suited to serve as probes as compared to the charmed mesons, in heavy-ion collision experiments (from the considerations of relaxation length). This may be perceived as a good news, considering the kind of impetus the first generation  $B$ –factory experiments has provided to  $b$ -physics. In recent years, both the BaBar experiment [46] at the PEP-II  $e^+e^-$  energy collider in SLAC, and the BELLE experiment [47, 48] at the KEKB  $e^+e^-$  energy collider, have utilized these respective high-luminosity experimental facilities to significantly improve the current understanding of bottom-flavored hadrons. The next generation  $B$ –factory experiments (BELLE-II [49], currently in the pipeline) are expected to enhance the experimental situation still further, considering a 40–fold increase in the instantaneous luminosity proposed in the SuperKEKB upgrade project of KEK [50, 51]. The observation of the hadrons with the heavy  $b$ -quark/antiquark has initiated studies of their in-medium behavior. One can easily reason on the basis of the strong density dependent medium effects already observed for the particles having light quark content, that corresponding medium effects for the  $B$  and  $\bar{B}$  mesons would also be substantial, due to similar light quark content. Therefore, for a full appreciation of the behavior of the  $B$  and  $\bar{B}$  mesons in such conditions, one must consider the effect of medium modifications of these mesons under such conditions. However, systematic treatments of such medium effects for these mesons have barely started pouring in, and there is need for more work on this subject. Apart from the works mentioned above, devoted specifically to the issue of their transport properties in the medium, there exist analyses of  $B$  meson in-medium behavior using the QCD Sum Rule method [11], and also using the quark meson coupling model [15]. Yasui and Sudoh have recently contributed considerably to this field, by analyzing the  $B$  meson properties within three different approaches – within heavy meson effective theory

with  $1/M$  corrections [52], by considering an effective Lagrangian for  $B - N$  interaction due to pion exchange [53], and especially the analysis of Ref.[54], where these were treated as heavy impurities embedded in a finite density medium, based on symmetry considerations. This third work [54], in particular, offers a unique perspective on this issue, as this physical situation is likened to the famous ‘Kondo problem’ in condensed matter physics. In the present work, we study the properties of the  $B(\bar{B})$  mesons in isospin asymmetric hyperonic matter at finite temperatures, arising from their interactions with the light hadrons in a chiral effective model.

We organize this article as follows: in section II, we outline the chiral  $SU(3)_L \times SU(3)_R$  model, and its subsequent generalization, used in this investigation. In section III, the Lagrangian density for the  $B$  and  $\bar{B}$  mesons, within this model, is explicitly written down and is used to derive their dispersion relations in the medium. In section IV, we describe and discuss what the preceding formulation implies for the in-medium properties of  $B$  and  $\bar{B}$  mesons and mention the possible implications of these medium effects. Finally, we summarize the findings of the present investigation in section V.

## II. THE CHIRAL EFFECTIVE MODEL

The current investigation is based on a generalization of the chiral  $SU(3)_L \times SU(3)_R$  model [24] designed for the light hadrons, to the heavy quark (charm and bottom) sector. A detailed exposition of the model can be found in Refs. [24, 25], but its main features are summarized here, for conciseness. This is a relativistic field theoretical model of interacting baryons and mesons, wherein the form of the interactions is dictated by chiral invariance. In this treatment, a nonlinear realization of chiral symmetry is adopted, which is in line with the approach successfully followed by Weinberg [55, 56] for the  $SU(2)_L \times SU(2)_R$  case. The same was generalized to arbitrary compact Lie groups and a general formulation for the construction of chiral-invariant Lagrangians was given in Refs. [57–59]. Also, the scale symmetry (invariance) which is broken in QCD, is introduced in the chiral model through a scalar dilaton field,  $\chi$  [60–62]. The expectation value of the dilaton field gets related to the expectation value of the scalar gluon condensate, as can be seen via a comparison of the trace of the energy-momentum tensor for the QCD case and for the chiral effective model [34–36, 60, 61]. It may be noted here that the scalar gluon condensate as calculated through the

chiral effective model [34–36] was used to calculate the mass shifts of the charmonium states through QCD second order Stark effect [36]. The effect of the twist 2 gluon condensates, as obtained from the medium change of the dilaton field calculated within the chiral effective model, on the in-medium masses of the  $J/\psi$  and  $\eta_c$ , has also been calculated using QCD sum rule approach [12]. The results obtained for the mass shifts of the charmonium states from the gluon condensates obtained within the chiral effective model, at low densities, were observed to be similar to as obtained using the gluon condensates of linear density approximation [37, 63].

The general expression for the Lagrangian density in this chiral effective model has the following form:

$$\mathcal{L} = \mathcal{L}_{\text{kin}} + \sum_W \mathcal{L}_{\text{BW}} + \mathcal{L}_{\text{vec}} + \mathcal{L}_0 + \mathcal{L}_{\text{scale break}} + \mathcal{L}_{\text{SB}} \quad (1)$$

In eqn.(1),  $\mathcal{L}_{\text{kin}}$  is the kinetic energy term.  $\mathcal{L}_{\text{BW}}$  is the baryon-meson interaction term, where the index  $W$  covers both spin-0 (scalar) and spin-1 (vector) mesons. Here, the baryon masses are generated dynamically, through the baryon-scalar meson interactions.  $\mathcal{L}_{\text{vec}}$  concerns the dynamical mass generation of the vector mesons through couplings with scalar mesons, apart from bearing the self-interaction terms of these mesons.  $\mathcal{L}_0$  contains the meson-meson interaction terms, and  $\mathcal{L}_{\text{scale break}}$  incorporates the scale invariance breaking of QCD through a logarithmic potential. Finally, the explicit symmetry breaking of  $U(1)_A$ ,  $SU(3)_V$  and chiral symmetry is incorporated in this effective hadronic model through the term  $\mathcal{L}_{\text{SB}}$ .

An analysis of the medium modifications of pseudoscalar mesons due to their interactions with the baryons (nucleons and hyperons) and scalar mesons, requires the assessment of the following contributions to the Lagrangian density -

$$\mathcal{L}_{\text{pseudoscalar}} = \mathcal{L}_{\text{WT}} + \mathcal{L}_{\text{SME}} + \mathcal{L}_{\text{1stRange}} + \mathcal{L}_{\text{d}_1} + \mathcal{L}_{\text{d}_2}, \quad (2)$$

where, the first term is the vectorial Weinberg-Tomozawa term, the second term arises due to the scalar meson exchange, and the last three terms are the range terms. The Weinberg-Tomozawa term corresponds to the leading order contribution, and, the scalar exchange term and range terms correspond to the the next to leading order contribution in the chiral perturbation expansion [29, 30, 34–36]. In the above, the Weinberg-Tomozawa term,  $\mathcal{L}_{\text{WT}}$  is given as -

$$\mathcal{L}_{\text{WT}} = -\frac{1}{2} \left[ \bar{B}_{ijk} \gamma^\mu \left( (\Gamma_\mu)_l^k B^{ijl} + 2 (\Gamma_\mu)_l^j B^{ilk} \right) \right], \quad (3)$$

where repeated indices are summed over. The same originates from the kinetic energy term ( $\mathcal{L}_{\text{kin}}$  in Eq. (1)) in the chiral model. The tensor  $B^{ijk}$ , which is antisymmetric in the first two indices, represents the baryons [8]. The indices  $i, j$  and  $k$  run from 1 to 5, and one can read off the quark/antiquark content of a baryon state,  $B^{ijk}$  as well as of the pseudoscalar mesons given as the matrix elements of the pseudoscalar matrix,  $M$  occurring in the expression  $\Gamma_\mu$  as given in the following, with the identification:  $1 \leftrightarrow u, 2 \leftrightarrow d, 3 \leftrightarrow s, 4 \leftrightarrow c, 5 \leftrightarrow b$ . However, in the current investigation, just like the charmed baryons [36], the medium modifications of the heavier (bottomed) baryons have not been accounted for, to study the in-medium properties of the  $B$  and  $\bar{B}$  mesons. In equation (3),  $\Gamma_\mu$  is defined as

$$\Gamma_\mu = -\frac{i}{4} \left[ \left( u^\dagger (\partial_\mu u) - (\partial_\mu u^\dagger) u \right) + \left( u (\partial_\mu u^\dagger) - (\partial_\mu u) u^\dagger \right) \right], \quad (4)$$

where the unitary transformation operator,  $u$ , is given as -

$$u = \exp \left( \frac{iM}{\sqrt{2}\sigma_0} \gamma_5 \right), \quad (5)$$

where  $M$  represents the matrix of pseudoscalar mesons, constructed as  $M = (M^a \lambda_a / \sqrt{2})$ , where  $M^a$  represents the field corresponding to  $a^{\text{th}}$  pseudoscalar meson, and the  $\lambda_a$ 's refer to the generalized Gell-Mann matrices.  $\mathcal{L}_{\text{SME}}$  is the scalar meson exchange term, which is obtained from the explicit symmetry breaking term ( $\mathcal{L}_{\text{SB}}$  in Eq. (1)) -

$$\mathcal{L}_{\text{SB}} = -\frac{1}{2} \text{Tr} \left( A_p \left( u X u + u^\dagger X u^\dagger \right) \right), \quad (6)$$

where,

$$A_p = \frac{1}{\sqrt{2}} \text{diag} \left[ m_\pi^2 f_\pi, m_\pi^2 f_\pi, \left( 2m_K^2 f_K - m_\pi^2 f_\pi \right), \left( 2m_D^2 f_D - m_\pi^2 f_\pi \right), \left( 2m_B^2 f_B - m_\pi^2 f_\pi \right) \right]. \quad (7)$$

The constants for the above expression are chosen so that, in conjunction with the fitted vacuum expectation values of the scalar fields, the PCAC relations are respected. The remaining terms in eqn.(2) are the range terms, which have the basic structure  $(\partial_\mu M)(\partial^\mu M)$ . The first range term is obtained from the kinetic energy term ( $\mathcal{L}_{\text{kin}}$  in Eq.(1)) of the pseudoscalar mesons in the chiral model [24], and goes as :

$$\mathcal{L}_{1^{\text{st}}\text{Range}} = \text{Tr}(u_\mu X u^\mu X + X u_\mu u^\mu X) \quad (8)$$

where  $u_\mu$  is defined in terms of the unitary transformation operator  $u$ , and its derivatives, as:

$$u_\mu = -\frac{i}{4} \left[ \left( u^\dagger (\partial_\mu u) - (\partial_\mu u^\dagger) u \right) - \left( u (\partial_\mu u^\dagger) - (\partial_\mu u) u^\dagger \right) \right], \quad (9)$$

The other two range terms in Eq.(2) are the  $d_1$  and  $d_2$  range terms, whose expressions are given below.

$$\mathcal{L}_{d_1} = \frac{d_1}{4} \left( \bar{B}_{ijk} B^{ijk} (u_\mu)_l^m (u^\mu)_m^l \right) \quad (10)$$

$$\mathcal{L}_{d_2} = \frac{d_2}{2} \left[ \bar{B}_{ijk} (u_\mu)_l^m \left( (u^\mu)_m^k B^{ijl} + 2(u^\mu)_m^j B^{ilk} \right) \right] \quad (11)$$

(repeated indices summed, as before). The  $d_1$  and  $d_2$  terms are the range terms which have been constructed from the baryon and pseudoscalar meson octets, within the chiral SU(3) model, to study the in-medium properties of the kaons and antikaons [30]. These terms were then generalized to SU(4) to study the D-mesons [34–36] and were written in the above form using the tensorial notations for the baryons as well as pseudoscalar mesons, since the baryons belong to a 20-plet and the mesons belong to 15-plet. In the present work, the interactions for the B mesons have been written down in a similar manner, including also the b-quarks. We make use of the mean field approximation [16, 25] to study hadron properties at finite densities and temperatures. Thus, we approximate for every scalar field  $\phi$  and vector field  $V^\mu$ ,

$$\phi \rightarrow \langle \phi \rangle \equiv \phi_0, \quad V^\mu (\equiv (V_0, \vec{V})) \rightarrow \langle V^\mu \rangle \equiv (V_0, 0), \quad (12)$$

where  $\phi_0$  and  $V_0$  are constants independent of space and time.  $X$ , occurring in eqns.(6) and (8), is the scalar meson multiplet, which in the mean field approximation, is given as,

$$X = \text{diag} \left[ \frac{(\sigma + \delta)}{\sqrt{2}}, \frac{(\sigma - \delta)}{\sqrt{2}}, \zeta, \zeta_c, \zeta_b \right] \quad (13)$$

In the above,  $\sigma (\sim (\bar{u}u + \bar{d}d))$ ,  $\zeta (\sim \bar{s}s)$ ,  $\zeta_c (\sim \bar{c}c)$ , and  $\zeta_b (\sim \bar{b}b)$  are the non-strange, strange, charmed and bottomed scalar-isoscalar mesons, and  $\delta (\sim (\bar{u}u - \bar{d}d))$  is the non-strange scalar-isovector meson. Within the mean field approximation, the equations of motion for the scalar and vector mesons, are derived, which are subsequently used in this investigation. It has been realized over a period of time, that this approximation, which is a vast simplification over the general case, is sufficient for a reasonable description of hadronic in-medium properties [25, 29–36]. We then write down the explicit expression for the Lagrangian density describing the interaction of the  $B$  and  $\bar{B}$  mesons with the light hadrons and the in-medium dispersion relations of the  $B$  and  $\bar{B}$  mesons obtained from this interaction Lagrangian density, in the next section.



### III. $B$ AND $\bar{B}$ MESONS IN HADRONIC MATTER

The Lagrangian density for the  $B$  and  $\bar{B}$  mesons in an isospin-asymmetric, strange, hadronic medium reads -

$$\mathcal{L}_{\text{total}}^B = \mathcal{L}_{\text{free}}^B + \mathcal{L}_{\text{int}}^B, \quad (14)$$

where this  $\mathcal{L}_{\text{free}}^B$  is simply the free Lagrangian density for the two pairs of complex scalar fields corresponding to the  $(B^+, B^-)$  and  $(B^0, \bar{B}^0)$  mesons:

$$\mathcal{L}_{\text{free}}^B = \left( \partial^\mu B^+ \right) \left( \partial_\mu B^- \right) - m_B^2 \left( B^+ B^- \right) + \left( \partial^\mu B^0 \right) \left( \partial_\mu \bar{B}^0 \right) - m_B^2 \left( B^0 \bar{B}^0 \right). \quad (15)$$

This  $\mathcal{L}_{\text{free}}^B$  can be recovered from the chiral model Lagrangian density in vacuum, from the expressions given by eqns.(6) and (8), by replacing  $X$  by its vacuum expectation value,  $X_0$ , as

$$\begin{aligned} \left( \mathcal{L}_{1^{\text{st}}\text{Range}}^B \right)_0 &= \left( \partial^\mu B^+ \right) \left( \partial_\mu B^- \right) + \left( \partial^\mu B^0 \right) \left( \partial_\mu \bar{B}^0 \right), \\ \left( \mathcal{L}_{\text{SME}}^B \right)_0 &= -m_B^2 \left( B^+ B^- + B^0 \bar{B}^0 \right). \end{aligned} \quad (16)$$

While the free Lagrangian density for the  $B$  mesons is borne out of these two terms in vacuum,

$$\mathcal{L}_{\text{free}}^B = \left( \mathcal{L}_{1^{\text{st}}\text{Range}}^B \right)_0 + \left( \mathcal{L}_{\text{SME}}^B \right)_0, \quad (17)$$

the finite density part of these two terms, given by eqns.(6) and (8), contribute to the interaction Lagrangian density.

The interaction Lagrangian density for the  $B$  and  $\bar{B}$  mesons, within this generalized chiral effective approach reads:

$$\mathcal{L}_{\text{int}}^B = \mathcal{L}_{\text{WT}}^B + \mathcal{L}_{\text{SME}}^B + \mathcal{L}_{\text{range}}^B, \quad (18)$$

where,

$$\begin{aligned} \mathcal{L}_{\text{WT}}^B &= \frac{-i}{8f_B^2} \left[ 3 \left( \bar{p} \gamma^\mu p + \bar{n} \gamma^\mu n \right) \left( ((\partial_\mu B^+) B^- - B^+ (\partial_\mu B^-)) + ((\partial_\mu B^0) \bar{B}^0 - B^0 (\partial_\mu \bar{B}^0)) \right) \right. \\ &\quad + \left( \bar{p} \gamma^\mu p - \bar{n} \gamma^\mu n \right) \left( ((\partial_\mu B^+) B^- - B^+ (\partial_\mu B^-)) - ((\partial_\mu B^0) \bar{B}^0 - B^0 (\partial_\mu \bar{B}^0)) \right) \\ &\quad + 2 \left( \bar{\Lambda} \gamma^\mu \Lambda + \bar{\Sigma}^0 \gamma^\mu \Sigma^0 \right) \left( ((\partial_\mu B^+) B^- - B^+ (\partial_\mu B^-)) + ((\partial_\mu B^0) \bar{B}^0 - B^0 (\partial_\mu \bar{B}^0)) \right) \\ &\quad + 2 \left( \bar{\Sigma}^+ \gamma^\mu \Sigma^+ + \bar{\Sigma}^- \gamma^\mu \Sigma^- \right) \left( ((\partial_\mu B^+) B^- - B^+ (\partial_\mu B^-)) + ((\partial_\mu B^0) \bar{B}^0 - B^0 (\partial_\mu \bar{B}^0)) \right) \\ &\quad + 2 \left( \bar{\Sigma}^+ \gamma^\mu \Sigma^+ - \bar{\Sigma}^- \gamma^\mu \Sigma^- \right) \left( ((\partial_\mu B^+) B^- - B^+ (\partial_\mu B^-)) - ((\partial_\mu B^0) \bar{B}^0 - B^0 (\partial_\mu \bar{B}^0)) \right) \\ &\quad + \left( \bar{\Xi}^0 \gamma^\mu \Xi^0 + \bar{\Xi}^- \gamma^\mu \Xi^- \right) \left( ((\partial_\mu B^+) B^- - B^+ (\partial_\mu B^-)) + ((\partial_\mu B^0) \bar{B}^0 - B^0 (\partial_\mu \bar{B}^0)) \right) \\ &\quad \left. + \left( \bar{\Xi}^0 \gamma^\mu \Xi^0 - \bar{\Xi}^- \gamma^\mu \Xi^- \right) \left( ((\partial_\mu B^+) B^- - B^+ (\partial_\mu B^-)) - ((\partial_\mu B^0) \bar{B}^0 - B^0 (\partial_\mu \bar{B}^0)) \right) \right], \quad (19) \end{aligned}$$

$$\mathcal{L}_{\text{SME}}^B = \frac{m_B^2}{2f_B} \left[ (\sigma' + \sqrt{2}\zeta'_b) (B^+ B^- + B^0 \bar{B}^0) + \delta (B^+ B^- - B^0 \bar{B}^0) \right] \quad (20)$$

$$\begin{aligned} \mathcal{L}_{\text{range}}^B = & \left( \frac{-1}{f_B} \right) \left[ (\sigma' + \sqrt{2}\zeta'_b) \left( (\partial^\mu B^+) (\partial_\mu B^-) + (\partial^\mu B^0) (\partial_\mu \bar{B}^0) \right) \right. \\ & \left. + \delta \left( (\partial^\mu B^+) (\partial_\mu B^-) - (\partial^\mu B^0) (\partial_\mu \bar{B}^0) \right) \right] \\ & + \frac{d_1}{2f_B^2} \left[ (\bar{p}p + \bar{n}n + \bar{\Lambda}\Lambda + \bar{\Sigma}^+ \Sigma^+ + \bar{\Sigma}^0 \Sigma^0 + \bar{\Sigma}^- \Sigma^- + \bar{\Xi}^0 \Xi^0 + \bar{\Xi}^- \Xi^-) \right. \\ & \quad \left. \times \left( (\partial_\mu B^+) (\partial^\mu B^-) + (\partial_\mu B^0) (\partial^\mu \bar{B}^0) \right) \right] \\ & + \frac{d_2}{4f_B^2} \left[ \left( 3(\bar{p}p + \bar{n}n) + 2(\bar{\Lambda}\Lambda + \bar{\Sigma}^0 \Sigma^0) + 2((\bar{\Sigma}^+ \Sigma^+ + \bar{\Sigma}^- \Sigma^-)) + (\bar{\Xi}^0 \Xi^0 + \bar{\Xi}^- \Xi^-) \right) \right. \\ & \quad \left. \times \left( (\partial_\mu B^-) (\partial^\mu B^+) + (\partial_\mu \bar{B}^0) (\partial^\mu B^0) \right) \right. \\ & \quad \left. + \left( (\bar{p}p - \bar{n}n) + 2(\bar{\Sigma}^+ \Sigma^+ - \bar{\Sigma}^- \Sigma^-) + (\bar{\Xi}^0 \Xi^0 - \bar{\Xi}^- \Xi^-) \right) \right. \\ & \quad \left. \times \left( (\partial_\mu B^-) (\partial^\mu B^+) - (\partial_\mu \bar{B}^0) (\partial^\mu B^0) \right) \right] \end{aligned} \quad (21)$$

In Eq. (18), the first term (with coefficient  $(-i/8f_B^2)$  as given by equation (19)) is the Weinberg-Tomozawa term, obtained from eqn.(3), the second term (with coefficient  $(m_B^2/2f_B)$  as given by equation (20)) is the scalar meson exchange term, obtained from the explicit symmetry breaking term of the Lagrangian (eqn.(6)), third term is the range term given by equation (21). The first range term (with coefficient  $-1/f_B$ ) is obtained from eqn.(8), and the other two range terms (with coefficients  $(d_1/2f_B^2)$  and  $(d_2/4f_B^2)$ , respectively) are the  $d_1$  and  $d_2$  terms, calculated from eqns.(10) and (11), respectively. Also,  $\sigma' (= \sigma - \sigma_0)$ ,  $\zeta'_b (= \zeta_b - \zeta_{b0})$ , and  $\delta' (= \delta - \delta_0)$  are the fluctuations of the respective scalar fields, from their vacuum expectation values. In writing down this form of the Lagrangian, we have left out all the cross (bilinear) terms (for example,  $\bar{p}\gamma^\mu n$ ,  $\bar{n}\gamma^\mu \Sigma^0$  etc.), since these do not contribute in the mean field limit. Additionally, from the transformation properties of Dirac bilinears, we recall that  $\rho^s = \bar{\psi}\psi$  is a scalar density, while the number density would be  $\rho = \psi^\dagger\psi = \bar{\psi}\gamma^0\psi$ , which is the zeroth component of the vector  $\bar{\psi}\gamma^\mu\psi$ . As we had mentioned earlier, in eqn.(12), in the mean field approximation, only the zeroth components of the vector fields contribute, that also as constants in space and time. Therefore, clubbing together the above arguments with eqn.(12), mean field approximation for the baryons in this context gives:

$$\bar{B}_i B_j \rightarrow \langle \bar{B}_i B_j \rangle \equiv \delta_{ij} \rho_i^s \quad (22)$$

$$\bar{B}_i \gamma^\mu B_j \rightarrow \langle \bar{B}_i \gamma^\mu B_j \rangle = \delta_{ij} \left( \delta_\mu^0 (\bar{B}_i \gamma^\mu B_j) \right) \equiv \delta_{ij} \rho_i \quad (23)$$

where the indices  $i$  and  $j$  cover the entire ‘baryon octet’ ( $p$ ,  $n$ ,  $\Lambda$ ,  $\Sigma^{\pm,0}$  and  $\Xi^{0,-}$ ). As mentioned previously as well, in the present investigation, we do not consider the effects of the still heavier (charmed and bottomed) baryons on the in-medium properties of the  $B$  and  $\bar{B}$  mesons. The scalar and number densities of the  $i$ -th baryon ( $i=p, n, \Lambda, \Sigma^{\pm,0}$  and  $\Xi^{0,-}$ ), occurring in eqns.(22-23), are given by the expressions:

$$\rho_i = \int d^3k (n_i(k) - \bar{n}_i(k)), \quad \rho_i^s = \int d^3k \frac{m_i^*}{E_i^*(k)} (n_i(k) + \bar{n}_i(k)), \quad (24)$$

where  $n_i(k)$  and  $\bar{n}_i(k)$  represent the particle and antiparticle distribution functions, given by -

$$n_i(k) \equiv n_i(k, \mu_i^*, T) = \frac{1}{\exp\left(\frac{E_i^* - \mu_i^*}{T}\right) \pm 1}, \quad \bar{n}_i(k) \equiv \bar{n}_i(k, \mu_i^*, T) = \frac{1}{\exp\left(\frac{E_i^* + \mu_i^*}{T}\right) \pm 1}. \quad (25)$$

In the above equations,  $m_i^*$  is the effective mass of the  $i^{th}$  baryon, given as -

$$m_i^* = - (g_{\sigma i} \sigma + g_{\zeta i} \zeta + g_{\delta i} \delta), \quad (26)$$

and  $\mu_i^*$  refers to the effective chemical potential of the  $i^{th}$  baryon, given by the expression

$$\mu_i^* = \mu_i - (g_{\rho i} \tau_3 \rho + g_{\omega i} \omega + g_{\phi i} \phi). \quad (27)$$

With the Lagrangian density obtained in the mean field approximation, we use the Euler-Lagrange equation to determine the equations of motion for the  $B$  and  $\bar{B}$  mesons. It can be readily observed from the form of the Lagrangian density, eqns.(16) and (18), that the equations of motion for  $B$  and  $\bar{B}$  mesons would come out to be linear. Therefore, by assuming plane wave solutions ( $\sim e^{i(\vec{k} \cdot \vec{r} - \omega t)}$ ), it is possible to ‘Fourier transform’ these equations of motion to obtain the in-medium dispersion relations for these mesons. These dispersion relations have the general form:

$$-\omega^2 + \vec{k}^2 + m_B^2 - \Pi(\omega, |\vec{k}|) = 0 \quad (28)$$

where,  $m_B$  is the vacuum mass of the respective  $B$  meson and  $\Pi(\omega, |\vec{k}|)$  is its *self-energy* in the medium, the latter representing the contribution of medium effects to the dispersion relations. The explicit expression for the self-energy  $\Pi(\omega, |\vec{k}|)$  for the  $B$  meson doublet ( $B^+$ ,

$B^0$ ), arising from the interaction of eqn.(18), is:

$$\begin{aligned}
\Pi(\omega, |\vec{k}|) = & \frac{-1}{4f_B^2} \left[ 3(\rho_p + \rho_n) \pm (\rho_p - \rho_n) + 2\rho_\Lambda + 2\rho_{\Sigma^0} + 2(\rho_{\Sigma^+} + \rho_{\Sigma^-}) \pm 2(\rho_{\Sigma^+} - \rho_{\Sigma^-}) \right. \\
& + (\rho_{\Xi^0} + \rho_{\Xi^-}) \pm (\rho_{\Xi^0} - \rho_{\Xi^-}) \left. \right] \omega + \frac{m_B^2}{2f_B} (\sigma' + \sqrt{2}\zeta_b' \pm \delta') \\
& + \left[ \frac{d_1}{2f_B^2} (\rho_p^s + \rho_n^s + \rho_\Lambda^s + \rho_{\Sigma^+}^s + \rho_{\Sigma^0}^s + \rho_{\Sigma^-}^s + \rho_{\Xi^0}^s + \rho_{\Xi^-}^s) \right. \\
& + \frac{d_2}{4f_B^2} \left( 3(\rho_p^s + \rho_n^s) \pm (\rho_p^s - \rho_n^s) + 2\rho_\Lambda^s + 2(\rho_{\Sigma^+}^s + \rho_{\Sigma^-}^s) \pm 2(\rho_{\Sigma^+}^s - \rho_{\Sigma^-}^s) \right. \\
& + 2\rho_{\Sigma^0}^s + (\rho_{\Xi^0}^s + \rho_{\Xi^-}^s) \pm (\rho_{\Xi^0}^s - \rho_{\Xi^-}^s) \left. \right) - \frac{1}{f_B} (\sigma' + \sqrt{2}\zeta_b' \pm \delta') \left. \right] (\omega^2 - |\vec{k}|^2) \quad (29)
\end{aligned}$$

where the  $+$  and  $-$  signs refer to the  $B^+$  and  $B^0$  mesons, respectively. Likewise, for the  $\bar{B}$  meson doublet ( $B^-$ ,  $\bar{B}^0$ ), the expression for self-energy is given as,

$$\begin{aligned}
\Pi(\omega, |\vec{k}|) = & \frac{1}{4f_B^2} \left[ 3(\rho_p + \rho_n) \pm (\rho_p - \rho_n) + 2\rho_\Lambda + 2\rho_{\Sigma^0} + 2(\rho_{\Sigma^+} + \rho_{\Sigma^-}) \pm 2(\rho_{\Sigma^+} - \rho_{\Sigma^-}) \right. \\
& + (\rho_{\Xi^0} + \rho_{\Xi^-}) \pm (\rho_{\Xi^0} - \rho_{\Xi^-}) \left. \right] \omega + \frac{m_B^2}{2f_B} (\sigma' + \sqrt{2}\zeta_b' \pm \delta') \\
& + \left[ \frac{d_1}{2f_B^2} (\rho_p^s + \rho_n^s + \rho_\Lambda^s + \rho_{\Sigma^+}^s + \rho_{\Sigma^0}^s + \rho_{\Sigma^-}^s + \rho_{\Xi^0}^s + \rho_{\Xi^-}^s) \right. \\
& + \frac{d_2}{4f_B^2} \left( 3(\rho_p^s + \rho_n^s) \pm (\rho_p^s - \rho_n^s) + 2\rho_\Lambda^s + 2(\rho_{\Sigma^+}^s + \rho_{\Sigma^-}^s) \pm 2(\rho_{\Sigma^+}^s - \rho_{\Sigma^-}^s) \right. \\
& + 2\rho_{\Sigma^0}^s + (\rho_{\Xi^0}^s + \rho_{\Xi^-}^s) \pm (\rho_{\Xi^0}^s - \rho_{\Xi^-}^s) \left. \right) - \frac{1}{f_B} (\sigma' + \sqrt{2}\zeta_b' \pm \delta') \left. \right] (\omega^2 - |\vec{k}|^2), \quad (30)
\end{aligned}$$

where, once again, the  $+$  and  $-$  signs refer to  $B^-$  and  $\bar{B}^0$  mesons, respectively. Additionally, we also study the optical potentials of these  $B$  and  $\bar{B}$  mesons in the present investigation, which are defined as,

$$U(\omega, k) = \omega(k) - \sqrt{k^2 + m_B^2} \quad (31)$$

where  $k$  ( $= |\vec{k}|$ ), is the momentum of the respective meson, and  $\omega(k)$  refers to its momentum dependent medium mass, obtained from the dispersion relation.

In the present work, we study the in-medium masses and the optical potentials of the  $B$  and  $\bar{B}$  mesons, which arise through the scalar and number densities of the baryons as well as the medium dependence of the scalar fields at given baryon density and temperature of the hadronic matter. The density and temperature dependence of the scalar fields are obtained by solving the coupled equations of motion of the scalar and vector fields. We also study the sensitivity of the medium modifications of these mesons, due to the isospin asymmetry as

well as strangeness of the hadronic matter, measured by the isospin asymmetry parameter,  $\eta$  and strangeness fraction,  $f_s$ . These parameters are defined as,  $\eta = -\sum_i(I_{3i}\rho_i)/\rho_B$ , where  $I_{3i}$  denotes the (third)  $z$  - component of isospin of the  $i^{th}$  baryon, and,  $f_s = \sum_i(|S_i|\rho_i)/\rho_B$ , where  $S_i$  is the strangeness quantum number of the  $i^{th}$  baryon. A detailed account of the dependence of the in-medium mass of the  $B$  and  $\bar{B}$  mesons on these parameters is given in the next section.

#### IV. RESULTS AND DISCUSSION

Before embarking on a description of what the above formulation entails for the in-medium properties of the  $B$  mesons in a hadronic environment, we first mention about the choice of parameters. The parameters of the chiral model are fitted to the vacuum masses of baryons, the nuclear saturation properties and other vacuum characteristics within the mean field approximation [24, 25]. In this investigation, we employ the same parameter set that has earlier been used to study kaons properties in hyperonic matter [30] as well as the open charmed ( $D$ ) mesons within this chiral model framework [36], and refer the interested reader to Refs.[24, 30, 36] for a detailed account of these fitting procedures. The parameters  $d_1$  and  $d_2$  are fitted to the empirical values of the low energy kaon-nucleon scattering lengths in the  $I=0$  and  $I=1$  channels [30–32]. For a further extension to the bottom sector, the only additional parameter required is the  $B$  meson decay constant,  $f_B$ , for which we use the value 190.6 MeV, consistent with the latest PDG [64]. We observe however, that this value is obtained [64] simply as an average over lattice QCD results [65, 66]. The value of  $f_B$  obtained using QCD Sum Rules [67–69] is slightly higher ( $\sim 207$  MeV), whereas the value of the  $B$ -decay constant typically taken in the literature [65, 66, 70–72] lies in the range of around 186 MeV to 197 MeV. We expect that the choice of a slightly different value of  $f_B$  will not make much difference to the results of the present investigation.

In Ref. [73], the behavior of quark condensates was studied for various  $U(N_f)_L \times U(N_f)_R$  linear sigma models, within the Hartree approximation, derived using the Cornwall-Jackiw-Tomboulis (CJT) formalism. Here,  $N_f$  denotes the number of quark flavors. Their model-independent analysis of the behavior of the light ( $N_f = 2$ ), strange ( $N_f = 3$ ) and charmed ( $N_f = 4$ ) quark condensates is invaluable for the generalization to another additional flavor, as is being considered here. It is observed that while there are substantial changes in the

light quark condensate, and a comparatively more subdued variation of the strange quark condensate, there is a near-constancy of the charmed quark condensate up to a temperature of around 200 MeV (with some exotic variation above this temperature). Since the effective field theoretical model used in our investigation constitutes a hadronic description of matter, we expect our model to give a reasonable description of reality, only as long as we have a hadronic phase in QCD. In light of the fact that above a pseudo-critical temperature  $T_c \approx 170$  MeV, QCD is predicted to go over to the deconfined regime [74–76], where we do not have hadrons, the constancy of charmed quark condensate, as obtained in [73], is thus expected to be valid over the entire hadronic regime of QCD. (The value of  $T_c$  quoted here originates from the calculations of the MILC collaboration [75]; a more recent computation by the HotQCD collaboration [76] predicts a smaller transition temperature ( $T_c = 154 \pm 9$  MeV), but that does not make any qualitative difference to the above conclusion.) This analysis has been used in support of the neglect of medium effects for the charmed condensate  $\langle \bar{c}c \rangle$ , in many works in the literature concerning the charmed mesons [33–36]. This also bodes well with expectations from physical grounds, since the mass of the charm quark is above the typical QCD energy scale ( $\sim 1$  GeV), below which non-perturbative approaches like our effective hadronic Lagrangian is considered appropriate [77]. However, since the mass of the bottom quark is still higher, it is reasonable to build on the analysis of Ref. [73], and treat the bottom degrees of freedom to be frozen in the medium as well. Consequently, for the entire numerical analysis in the present investigation, we neglect the medium effects on the  $B$  and  $\bar{B}$  mesons due to the bottom condensate  $\langle \bar{b}b \rangle$ . More specifically, we neglect the variation of the bottomed scalar field ( $\zeta_b$ ) from its vacuum value and set  $\zeta_b' = \zeta_b - \zeta_{b0} \equiv 0$  in the current investigation.

We now analyze the in-medium behavior of  $B$  and  $\bar{B}$  mesons, as per the formulation of the previous section. The contributions of the various individual interaction terms to the total in-medium masses of the  $B$  and  $\bar{B}$  mesons are shown in Fig. 1, for isospin symmetric ( $\eta = 0$ ) nuclear ( $f_s = 0$ ) as well as hyperonic matter, with  $f_s = 0.5$ . In symmetric matter, the scalar meson exchange term gives an attractive contribution to all four of these  $B$  and  $\bar{B}$  mesons, hence lowering their medium mass. This can be understood by realizing that since  $\zeta_b$  is being treated as frozen and the value of the scalar-isovector field  $\delta$  is zero in the symmetric situation, the entire variation of this interaction term is due to the fluctuations of the scalar-isoscalar  $\sigma$  field. The behavior of these scalar fields in this chiral effective model,

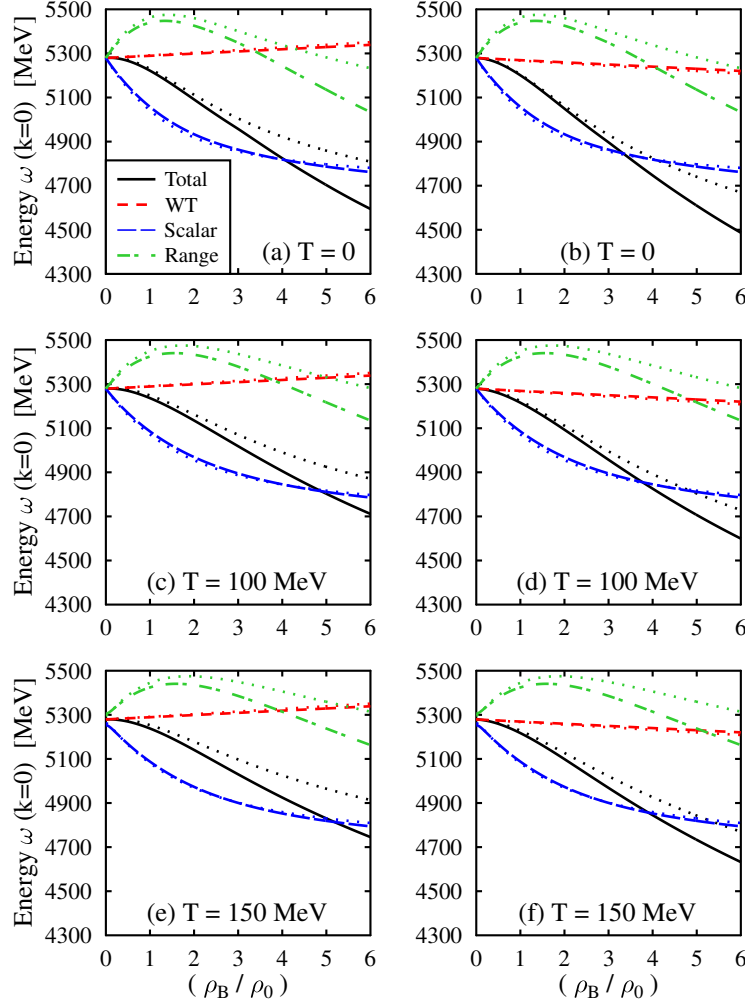


FIG. 1. (Color Online) The various contributions to the energy at  $\vec{k} = 0$ , for the  $B$  and  $\bar{B}$  mesons in isospin symmetric matter ( $\eta = 0$ ), at different temperatures. Subplots (a), (c) and (e) correspond to the degenerate  $B$  mesons ( $B^+$ ,  $B^0$ ), while (b), (d) and (f) correspond to the degenerate  $\bar{B}$  mesons ( $B^-$ ,  $\bar{B}^0$ ). For each case, the individual contributions in hyperonic matter (with  $f_s = 0.5$ ), as described in the legend, are also compared against the nuclear matter situation ( $f_s = 0$ ), represented by dotted curves.

in both nuclear and hyperonic matter situations, has been studied in detail in Refs. [35, 36]. It is observed that  $\sigma' = \sigma - \sigma_0 > 0$  at all finite densities, hence, it follows from eqns. (29) and (30) that the contribution of this term is attractive, for the entire range of density variation considered here. On the other hand, the behavior of the total range term, which is the sum of the contributions from the  $d_1$  range term,  $d_2$  range term and the first range term, is quite

non-trivial. It is observed that the total contribution of these range terms is repulsive till a density of about  $1.5\rho_0$ ; thereafter, it becomes attractive and contributes further to a lowering of the in-medium mass for the  $B$  and  $\bar{B}$  mesons. This kind of behavior arises because of the interplay of the repulsive first range term and the attractive  $d_1$  and  $d_2$  range terms. It follows from their respective expressions that while the density dependence of the first range term is because of the  $\sigma$  field in this symmetric matter situation, that for the other two range terms is through scalar densities of the nucleons and the hyperons. While the relation  $\sigma' \approx \rho^s$  holds approximately for smaller densities, at larger densities, there is considerable departure from this approximate equality and the density dependence of  $\sigma$  is significantly sub-linear, becoming progressively more and more sluggish as we go to higher densities. On the other hand, scalar densities of all eight baryons increase monotonically with  $\rho_B$ . Thus, it is inevitable that these progressively growing attractive contributions, though initially smaller, would predominate over the decreasing magnitude of the repulsive first range term, which explains the observed behavior of the range terms.

It follows from the eqn.(29) that the isospin pair constituted by the two  $B$  mesons ( $B^+$ ,  $B^0$ ) is degenerate in isospin symmetric matter, irrespective of the value of  $f_s$ . (In making this assertion, we are neglecting the small 0.33 MeV difference in their vacuum masses [64], since this number is much smaller than the typical magnitude of their mass shifts that we are concerned with.) This is because symmetric matter not only has an equal number of isospin-pair-baryons,  $(p, n)$ ,  $(\Sigma^+, \Sigma^-)$ ,  $(\Xi^0, \Xi^-)$ , but also, the scalar-isovector field  $\delta$  vanishes. With this, the asymmetric contributions to the Weinberg-Tomozawa term and the  $d_2$  range term vanish, while the first range term contributes equally to the isospin doublets, just like the scalar meson exchange term which was addressed before. The  $d_1$  range term is anyways common for all four mesons, even in the asymmetric situation, as can be seen explicitly from the self-energy expressions. Similar to the masses of the  $B^+$  and  $B^0$ , which are identical in symmetric matter, the masses of the  $B^-$  and  $\bar{B}^0$  also remain same in isospin symmetric matter at finite densities. In vacuum, the masses of  $B^+$  and  $B^0$  coincide with the masses of  $B^-$  and  $\bar{B}^0$ . This, however is no longer the case at finite densities. For example, in cold ( $T = 0$ ) nuclear matter, the values of the mass drop  $\Delta m = (m_{\text{vacuum}} - m_{\rho_B})$  for the  $B$  and  $\bar{B}$  mesons at  $\rho_B = \rho_0$  are 49 and 74 MeV respectively, which grow to 165 and 217 at  $2\rho_0$  and, 357 and 454 MeV respectively, at  $4\rho_0$ . This difference arises because, the isospin symmetric part of the vectorial Weinberg-Tomozawa interaction has equal and opposite contributions



for these antiparticle pairs, as can be seen explicitly from the expressions for their self-energies. Being repulsive for the  $B$  mesons (subplots (a), (c) and (e) in Fig.1) and attractive for the  $\bar{B}$  mesons (subplots (b), (d) and (f)), this interaction term leads to an extra drop in the medium mass for the latter as compared to the former.

As we go from symmetric nuclear to symmetric hyperonic matter, i.e. increase the value of  $f_s$ , the in-medium mass of both  $B$  and  $\bar{B}$  mesons is observed to decrease. For example, the 49 and 74 MeV mass drops for the  $B$  and  $\bar{B}$  mesons respectively, at  $\rho_B = \rho_0$  in cold nuclear matter mentioned earlier, grow to 57 and 78 MeV respectively, for cold hyperonic matter with  $f_s = 0.5$ . The mass drops for these two sets of mesons are 198 and 231 at  $2\rho_0$  and, 454 and 532 MeV respectively at  $\rho_B = 4\rho_0$  in the  $f_s = 0.5$  situation, which are significantly higher than the corresponding numbers in nuclear matter (165 and 217 for  $2\rho_0$  and 357 and 454 MeV at  $4\rho_0$ , as mentioned before). To understand this overall decrease, we must analyze the effects of increasing  $f_s$  on each of these individual contributions to the total in-medium mass. It is established [36] that  $\sigma$  increases in magnitude with an increase in  $f_s$  up to a certain density (e.g.  $\sim 3.9\rho_0$  in the  $T = 0$  situation), beyond which it starts decreasing. As we had noted previously, the entire variation of the scalar meson exchange term is because of this  $\sigma$  field in symmetric matter; hence, its behavior is exactly in accordance with that of  $\sigma$ . In particular, it can be clearly discerned that, for the  $T = 0$  case for example, while the contribution from this term for the hyperonic ( $f_s = 0.5$ ) matter case is smaller in magnitude as compared to that for the nuclear matter for  $\rho_B < 3.9\rho_0$ , a reversal occurs for densities higher than this. This reversal, and especially the precise value of crossover point, is exactly in accordance with the observed behavior for the  $\sigma$  field. The same reasoning extends over to the the magnitude of the (repulsive) first range term, though there is no such reversal for the total range term. This is so, because of the contributions from the  $d_1$  and  $d_2$  range terms, which are totally dependent on the scalar densities. As was reasoned already, the decreasing magnitude of the  $\sigma$  dependent repulsive contribution makes it inevitable that the large density behavior of the total range terms would be governed by these attractive,  $\rho^s$ -dependent interaction terms. Now, the effect of increasing  $f_s$  on the  $d_1$  range term is to increase the magnitude of the attractive interactions at larger densities. This result appears surprising at first glance, since this  $d_1$  range term depends only on the sum of all eight scalar densities,  $(\sum_i \rho_i^s)$ . By increasing  $f_s$ , we are only redistributing the total density amongst these eight species, so one may naively expect the sum to remain the same

irrespective of the value of  $f_s$ . However, this is not the case, since this process redistributes the total number density ( $\rho_B = \sum_i \rho_i$ ), and not the scalar density, for which there is no such overall conservation. While  $\rho_B^s \approx \rho_B$  at small densities, at larger densities, the former, though still an increasing function, has much more subdued increase with respect to the latter. The fact that they are identical at small densities, implies an approximate overall conservation at small densities, in line with the above reasoning, which is indeed observed to be the case. Thus, while this interaction term has a negligible  $f_s$  dependence till  $\rho_B \approx \rho_0$ , there is a considerable increase in its magnitude at larger densities, with an increase in  $f_s$ . On the other hand, the  $f_s$  dependence of  $d_2$  range term is comparatively less pronounced, and has the exactly opposite behavior - this term is observed to increase with  $f_s$  till about  $5\rho_0$  and show a marginal increase thereafter. Naturally then, the larger magnitude of the  $d_1$  range term dominates over the other two, and the overall behavior of range terms is to decrease with  $f_s$ . This is especially pronounced at larger densities, where it is responsible for causing a still larger decrease in the medium mass for the  $B$  and  $\bar{B}$  mesons. Lastly, the Weinberg-Tomozawa term is known to decrease in magnitude as the value of  $f_s$  is increased, which can be inferred by repeating the argument, presented for  $D(\bar{D})$  mesons in Ref. [36]. It follows from eqns. (29) and (30), that in symmetric nuclear matter, the magnitude of this interaction term is proportional to  $(3(\rho_p + \rho_n))$ , which would imply a precisely linear increase (or decrease, for the corresponding antiparticle) with density, since  $\rho_B = (\rho_p + \rho_n)$  in nuclear matter. However, in symmetric hyperonic matter, the total  $\rho_B$  is redistributed amongst all eight baryons, such that the magnitude of this interaction term is proportional to  $(3(\rho_p + \rho_n) + 2(\rho_\Lambda + \rho_{\Sigma^0} + \rho_{\Sigma^+} + \rho_{\Sigma^-}) + \rho_{\Xi^0} + \rho_{\Xi^-})$ , which can be rearranged in a more illuminating form, as  $(3\sum_i \rho_i - (\rho_\Lambda + \rho_{\Sigma^0} + \rho_{\Sigma^+} + \rho_{\Sigma^-} + 2(\rho_{\Xi^0} + \rho_{\Xi^-})))$ . Recognizing that the first term itself equals  $\rho_B$ , this factor is of the form  $(3\rho_B - g(\rho, f_s))$ , where the term  $g$ , being totally dependent on the hyperonic number densities, is an increasing function of both  $f_s$  and  $\rho_B$ . It follows then, that the magnitude of this Weinberg-Tomozawa term decreases with  $f_s$  for fixed  $\rho_B$ , and with  $\rho_B$  for fixed  $f_s$ , which is in exact agreement with what one observes from Fig. 1.

Naturally then, the cumulative effect of all that has been reasoned above, is to decrease the in-medium mass of these four mesons, in hyperonic matter as compared to nuclear matter. Additionally, it may be observed from Fig. 1 that while  $B$  and  $\bar{B}$  mesons are still non-degenerate, the magnitude of mass-asymmetry between antiparticles reduces with  $f_s$ .

For example, the values of  $(m_B, m_{\bar{B}})$  in cold hyperonic matter at  $\rho_B = \rho_0$ , are (5222, 5201), (5091, 5049) and (4825, 4747) MeV respectively, 5 at  $\rho_B = \rho_0$ ,  $\rho_B = 2\rho_0$  and  $4\rho_0$  respectively (hence implying  $B - -\bar{B}$  mass difference of 21, 42 and 78 MeV, respectively), as against the values of (5230, 5205), (5112, 5062), and (4922, 4825) MeV, respectively, ( $B - -\bar{B}$  mass difference 25, 50 and 97 MeV, respectively) in cold nuclear matter. This follows immediately from the reasoning of the previous paragraph, since we had noted earlier that it is the Weinberg-Tomozawa term that is responsible for a mass shift asymmetry between particle and antiparticle. Thus, a decrease in the magnitude of this interaction term with  $f_s$ , ought to have this effect.

To conclude our discussion of symmetric matter, we depart from our treatment of cold ( $T = 0$ ) matter and consider the effect of a finite temperature on the in-medium mass of these mesons. It is observed that respective magnitudes of the mass drops for both  $B$  and  $\bar{B}$  mesons decrease at larger temperatures. For example, in symmetric nuclear matter, the  $T = 0$  mass drops of 167 and 217 at  $\rho_B = 2\rho_0$ , and, 357 and 454 MeV at  $\rho_B = 4\rho_0$  mentioned earlier for the  $B$  and  $\bar{B}$  mesons respectively, shrink to 117 and 168 for  $2\rho_0$  and 289 and 387 MeV for  $4\rho_0$ , respectively at  $T = 100$  MeV, and further to 101 and 152 for  $\rho_B = 2\rho_0$ , and, 253 and 353 MeV for  $\rho_B = 4\rho_0$  at  $T = 150$  MeV. Likewise, for strange hadronic matter with  $f_s = 0.5$ , the corresponding  $T = 0$  mass drops of 188 and 250 at  $\rho_B = 2\rho_0$ , and, 454 and 532 MeV at  $\rho_B = 4\rho_0$ , are observed to reduce to 144 and 186 for  $\rho_B = 2\rho_0$ , and, 374 and 453 MeV respectively at  $\rho_B = 4\rho_0$ , at  $T = 100$  MeV, and further to 138 and 180 for  $\rho_B = 2\rho_0$  and, 354 and 434 MeV for  $\rho_B = 4\rho_0$ , at  $T = 150$  MeV. This decrease in the mass shifts as the temperature is raised, originates due to a decrease in the magnitudes of the scalar fields with increase in temperature. The weakening of the medium effects with an increase in temperature has earlier been observed for kaons and antikaons [28] and  $D$  mesons [33, 35, 36] within the chiral effective model.

Everything considered so far in this discussion pertained to isospin-symmetric matter ( $\eta = 0$ ). We now proceed to discuss the behavior of  $B$  and  $\bar{B}$  mesons in the more general situation of isospin asymmetric matter. Figures 2 and 3 show the behavior of in-medium mass of the  $B$  mesons ( $B^+$ ,  $B^0$ ) and the  $\bar{B}$  mesons ( $B^-$ ,  $\bar{B}^0$ ) respectively, in both nuclear and hyperonic matter ( $f_s = 0.5$ ) situations, along with the various individual contributions to the total in-medium mass of the  $B$  and  $\bar{B}$  mesons, in asymmetric matter with  $\eta = 0.5$ . The particles constituting the isospin doublets are observed to be non-degenerate in isospin-

asymmetric matter. This disparity is evident in figures 2 and 3, from which one can easily see that the mass of  $B^0$  meson drops more than that of  $B^+$  meson, and that of  $\bar{B}^0$  meson drops more than the  $B^-$  meson. This behavior originates from the fact that the asymmetric contributions to the in-medium interactions, which are now non-zero, distinguish between these isospin pairs. For example, in the nuclear matter situation, the Weinberg-Tomozawa term has an extra asymmetric contribution of  $\pm(\rho_p - \rho_n)$ , which makes this interaction term more repulsive for  $B^0$  meson as compared to the  $B^+$  meson. Likewise, this additional term makes this term more attractive for  $\bar{B}^0$  meson as compared to  $B^-$  meson, hence decreasing further the in-medium mass of the  $\bar{B}^0$  meson. In hyperonic matter, this Weinberg-Tomozawa term also has asymmetric contributions from similar terms dependent on the hyperonic number densities. Due to exactly the same structure of interaction terms, albeit in terms of scalar densities, a similar reasoning applies to the  $d_2$  range term. Additionally, the respective contributions of the scalar meson exchange term and the (repulsive) first range term also differ for these isospin pairs, owing to a  $(\sigma \pm \delta)$  structure in the interaction terms, as can be seen from eqns. (29) and (30). In fact, even the  $d_1$  range term, which appears to be completely isospin symmetric (since it is proportional to  $\sum_i \rho_i^s$ ), gets altered in magnitude as compared to the  $\eta = 0$  situation. This difference arises because the values of the scalar fields calculated with  $\delta = 0$  in the symmetric situation, turn out to be different from those calculated in the asymmetric situation, with  $\delta \neq 0$ . These values of the scalar fields are then used to calculate the scalar densities, which are, thus, altered between these two cases. Thus, it can be inferred that the entire behavior of the individual terms, and hence, also their interplay, is entirely different in isospin-asymmetric situation, as compared to the symmetric case.

Thus, realizing that even in this most general situation, the behavior of the in-medium mass of  $B$  and  $\bar{B}$  mesons can be understood by studying this interplay of individual contributions, we proceed to discuss the cumulative sensitivity of their medium mass on each of these four parameters  $(\rho_B, T, \eta, f_s)$ , as is shown in figures 4 - 7. These show the comparative behavior of these mesons in both nuclear and hyperonic matter, in both symmetric and asymmetric situations, as a function of density, and at various temperatures. In order to make the effects of asymmetry and strangeness clearer from the outset, we have concerned ourselves with rather extreme values of these parameters in figures 1 - 3, where the only values of these parameters considered were 0 and 0.5. However, the physical situation in

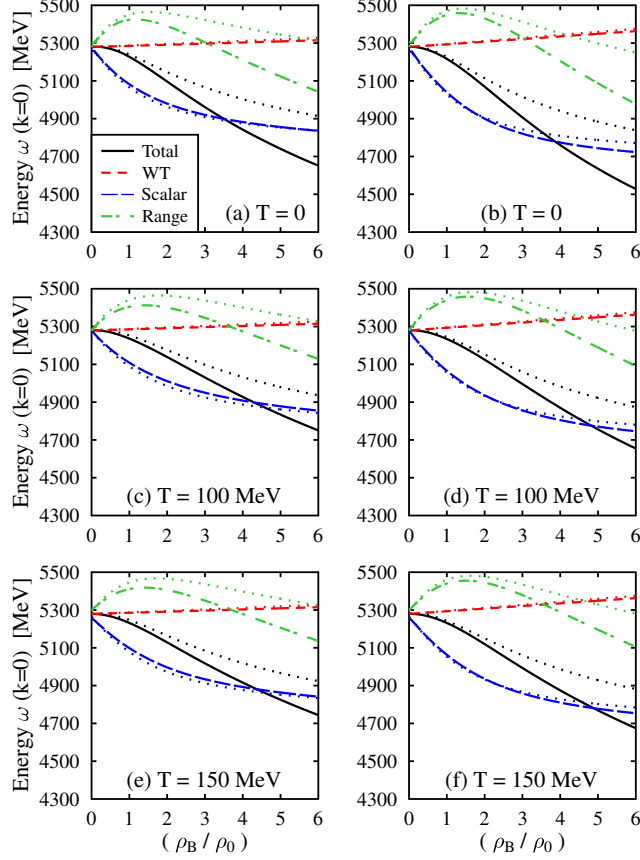


FIG. 2. (Color Online) The various contributions to the energy at  $\vec{k} = 0$ , for the  $B$  meson doublet ( $B^+$ ,  $B^0$ ) in isospin asymmetric matter ( $\eta = 0.5$ ), at different temperatures. Subplots (a), (c) and (e) correspond to the  $B^+$  meson while (b), (d) and (f) correspond to the  $B^0$  meson. For each case, the individual contributions in hyperonic matter (with  $f_s = 0.5$ ), as described in the legend, are also compared against the nuclear matter situation ( $f_s = 0$ ), represented by dotted curves.

typical experimental situations is comparatively, more modest. For example, the isospin asymmetry in collision experiments involving lead ( $^{207}\text{Pb}_{82}$ ) and gold ( $^{197}\text{Au}_{79}$ ) nuclei may be estimated from the isospin asymmetry in these nuclei themselves, to a first approximation. The same comes out to be roughly  $\eta \approx 0.2$  for both cases. Likewise, since the hyperons are more massive as compared to nucleons, it is not unrealistic at all to expect them to be less abundant than the latter in typical situations, which implies that the possibility of a less extreme value of  $f_s$  should also be entertained. Since each of these parameter values are fed in as inputs into our calculations of the medium mass, these intermediate cases can

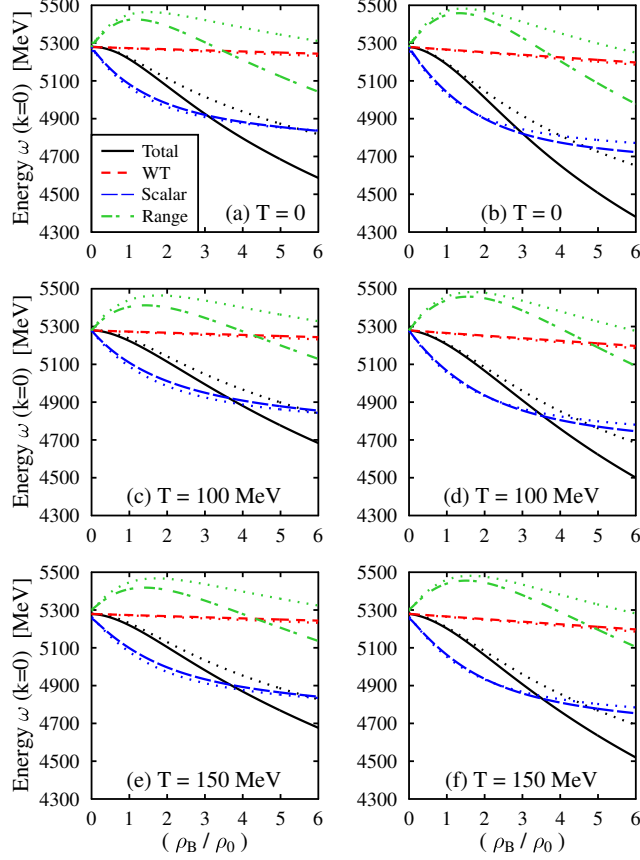


FIG. 3. (Color Online) The various contributions to the energy at  $\vec{k} = 0$ , for the  $\bar{B}$  meson doublet ( $B^-$ ,  $\bar{B}^0$ ) in isospin asymmetric matter ( $\eta = 0.5$ ), at different temperatures. Subplots (a), (c) and (e) correspond to the  $B^-$  meson while (b), (d) and (f) correspond to the  $\bar{B}^0$  meson. For each case, the individual contributions in hyperonic matter (with  $f_s = 0.5$ ), as described in the legend, are also compared against the nuclear matter situation ( $f_s = 0$ ), represented by dotted curves.

be similarly covered, and are also included in the discussion that follows. While everything reasoned thus far in this article, be it the fact that the mass drops intensify on the addition of hyperons in the medium, or that (in general) the mass drops weaken at higher temperatures, or the degeneracy and degeneracy breaking inferred already, is nicely reflected in figures 4 - 7, these make explicit the effect of isospin asymmetry on the in-medium mass of the  $B$  and  $\bar{B}$  mesons. Since we had clamped  $\eta$  to a fixed value even while addressing their effective mass in the asymmetric situation in figures 2 and 3, we now analyze the effect of increasing  $\eta$  on the in-medium mass of these mesons. We begin with the hyperonic matter ( $f_s = 0.3$

situation in figures 4 - 5, and  $f_s = 0.5$  situation in figures 6 - 7) and address the somewhat anomalous nuclear matter situation a little later. One can readily observe that in hyperonic matter, for each pair of isospin doublets, the effect of increase in asymmetry is opposite - producing a decrease in mass for one meson, and an increase for the other. This is absolutely consistent with what we have already observed in the individual terms - the opposite nature of asymmetric contributions for  $B^+$  and  $B^0$  meson (as well as for the corresponding  $\bar{B}$  mesons ( $B^-$  and  $\bar{B}^0$ )). While the symmetric parts of each of these individual contributions is common for these isospin pairs and contribute to identical decrease with density, these asymmetric contributions in Weinberg-Tomozawa term,  $d_2$  range term, as well as the  $(\sigma' \pm \delta')$  structure in the first range term as well as the scalar meson exchange term, are responsible for causing a further drop for the  $B^0$  and  $\bar{B}^0$  mesons, and a relative increase in the medium mass for  $B^+$  and  $B^-$ , as compared to the symmetric situation. Further, it is observed that, in general, this isospin dependence decreases at larger temperatures, which is due to a decrease in the magnitude of  $\delta$  at larger temperatures, hence producing a decrease in the magnitude of each of these asymmetric contributions. In nuclear matter, however, it is observed that while isospin asymmetry produces an increase and decrease, respectively, in the  $B^-$  and  $\bar{B}^0$  meson mass (just like the hyperonic matter situation), the  $B$  meson doublet has an apparently anomalous behavior. Here, the  $B^+$  meson mass is observed to increase with asymmetry, the magnitude of isospin dependence decreasing with temperature, just like the finite  $f_s$  situation. However, the  $B^0$  meson mass is observed to show a small increase with asymmetry in the  $T = 0$  situation, while at larger temperatures, one encounters a reversal in this behavior, with the effective mass exhibiting a small decrease with asymmetry. It may be noted in particular that the magnitude of temperature dependence of  $B^0$  mass is the weakest out of all four mesons, due to this gradual reversal in sign at intermediate temperatures. This apparent discrepancy is once again due to a delicate interplay between the consistently attractive scalar meson exchange term contribution, the consistently repulsive Weinberg-Tomozawa term contribution and the contribution from the range terms which switch from repulsive to attractive at larger densities. At smaller temperatures, in the asymmetric situation, one observes that these contributions almost counterbalance each other at small densities, hence producing a resultant of small magnitude. At larger densities, aided by the extra asymmetric terms, the contribution from the Weinberg-Tomozawa term is observed to dominate over the other (attractive) contributions, hence producing a net increase in

mass with asymmetry. At larger temperatures, however, the magnitude of scalar field  $\sigma$  increases, while the magnitude of  $\delta$  decreases, which implies that both the fluctuations in  $\sigma$  and  $\delta$  decrease in magnitude, hence disturbing this delicate balance. This has a larger effect on the attractive scalar meson exchange term and total range term, as compared to the relatively robust Weinberg-Tomozawa term, with the result that the overall magnitude of the attractive terms increases over that of the repulsive contributions, producing a net decrease in mass with asymmetry at higher temperatures. Additionally, it can be discerned that between these four mesons,  $\bar{B}^0$  meson suffers the largest magnitude of mass drop in asymmetric hyperonic matter situation. This follows from the fact that, as has already been mentioned that  $\bar{B}$  mesons have a larger mass drop as compared to  $B$  mesons, which intensifies further in hyperonic matter situation. Adding to this the fact that  $B^0$  and  $\bar{B}^0$  masses drop further in asymmetric matter, it follows that for  $\bar{B}^0$  meson, the effect of decrease in medium mass with  $f_s$  gets accentuated by a decrease with isospin asymmetry parameter, hence producing the acute mass drop for  $\bar{B}^0$ , as compared to the other mesons ( $B^\pm$ ,  $B^0$ ).

As has been reasoned already, in asymmetric matter, the effect of the extra asymmetric terms is to make the Weinberg-Tomozawa term more repulsive for  $B^0$  meson as compared to the  $B^+$  meson, and more attractive for the  $\bar{B}^0$  meson as compared to the  $B^-$  meson. It may be noticed from the expressions of the in-medium self energies that while these extra asymmetric contributions break the mass degeneracy of isospin doublets as was seen above, the mass degeneracy of antiparticles ( $B^+$ ,  $B^-$ ) and ( $B^0$ ,  $\bar{B}^0$ ) is still getting broken because of equal and opposite contributions of this Weinberg-Tomozawa term only. Putting these two factors together, it follows that the magnitude of mass shift asymmetry between ( $B^0$ ,  $\bar{B}^0$ ) is larger than that between ( $B^+$ ,  $B^-$ ), as can be seen from figures 2 and 3. For example, in cold hyperonic matter, with  $f_s = 0.5$ , the values of  $(\Delta m_{B^+}, \Delta m_{B^-})$  are observed to be (52, 64), (182, 207) and (437, 483) MeV, at  $\rho_B = \rho_0$ ,  $2\rho_0$  and  $4\rho_0$  respectively. These may be compared to the numbers (63, 92), (210, 268) and (519, 626) MeV for the  $(\Delta m_{B^0}, \Delta m_{\bar{B}^0})$  mesons under the same conditions. We might note here that the corresponding values in the symmetric situation, (57, 78), (188, 230) and (454, 532) MeV for the  $B$  and  $\bar{B}$  mesons,  $(\Delta m_B, \Delta m_{\bar{B}})$  at densities of  $\rho_0$ ,  $2\rho_0$  and  $4\rho_0$  respectively, were identical for the two pairs, since both the  $B$  mesons and both the  $\bar{B}$  mesons were degenerate in that situation. Since all other contributions, even with the extra asymmetric contributions, are exactly identical for antiparticles, this behavior is completely borne out of the larger magnitude of the contribution



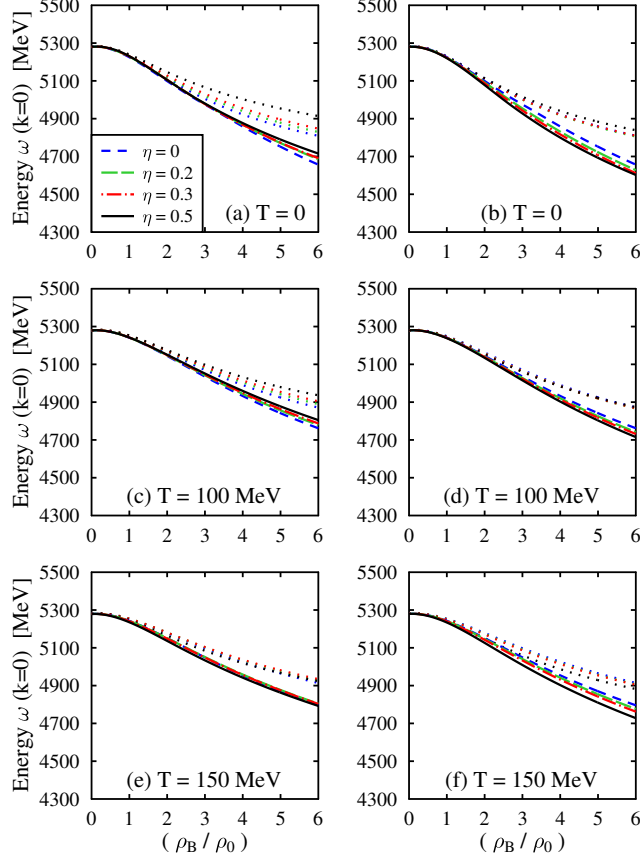


FIG. 4. (Color Online) A comparison of the energy at  $\vec{k} = 0$ , of the  $B^+$  (subplots (a), (c) and (e)) and  $B^0$  mesons (subplots (b), (d) and (f)), in hyperonic matter (with  $f_s = 0.3$ ), at various values of the isospin asymmetry parameter ( $\eta$ ), as described in the legend, and at different temperatures. In each case, this hyperonic matter situation is also compared against the nuclear matter ( $f_s = 0$ ) situation, represented by dotted lines.

from this Weinberg-Tomozawa term for the antiparticle pair ( $B^0, \bar{B}^0$ ) as compared to ( $B^+, B^-$ ). Also, it clearly follows from figures 4 - 7 that the variation of medium mass for either meson with both isospin asymmetry parameter and strangeness is completely monotonic, since the mass drops corresponding to intermediate values of these parameters (which, as we saw earlier, are more realistic choices from the point of view of experimental relevance) are also intermediate between the two extreme situations considered by us, for either of these parameters.

Building on this analysis of the effective mass of  $B$  and  $\bar{B}$  mesons, we now depart from

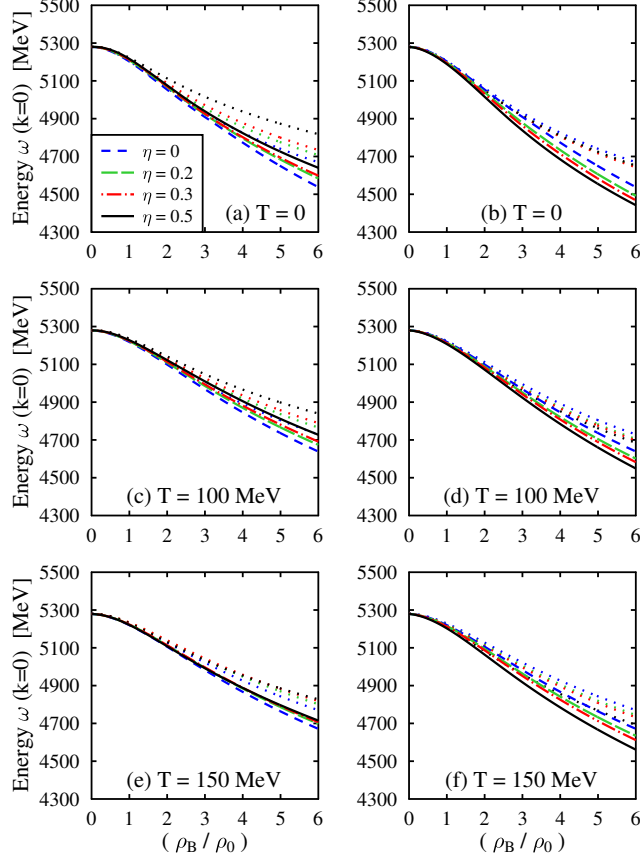


FIG. 5. (Color Online) A comparison of the energy at  $\vec{k} = 0$ , of the  $B^-$  (subplots (a), (c) and (e)) and  $\bar{B}^0$  mesons (subplots (b), (d) and (f)), in hyperonic matter (with  $f_s = 0.3$ ), at various values of the isospin asymmetry parameter ( $\eta$ ), as described in the legend, and at different temperatures. In each case, this hyperonic matter situation is also compared against the nuclear matter ( $f_s = 0$ ) situation, represented by dotted lines.

the line of approach followed so far in this article, where we have considered the medium effects at  $\vec{k} = 0$ , and venture into the finite momentum regime. To this end, we consider the in-medium optical potentials for the  $B$  and  $\bar{B}$  mesons, defined via eqn.(31). Figures 8-11 show the variation of optical potentials of  $B$  and  $\bar{B}$  mesons with momentum  $k$  ( $= |\vec{k}|$ ), at  $\rho_B = \rho_0, 2\rho_0$  and  $4\rho_0$ , in both symmetric and asymmetric, nuclear and hyperonic matter at  $T = 0$ . In order to appreciate this behavior of optical potentials, we note that as per its definition (31), at  $k = 0$ , optical potential is just the negative of the mass drop of the

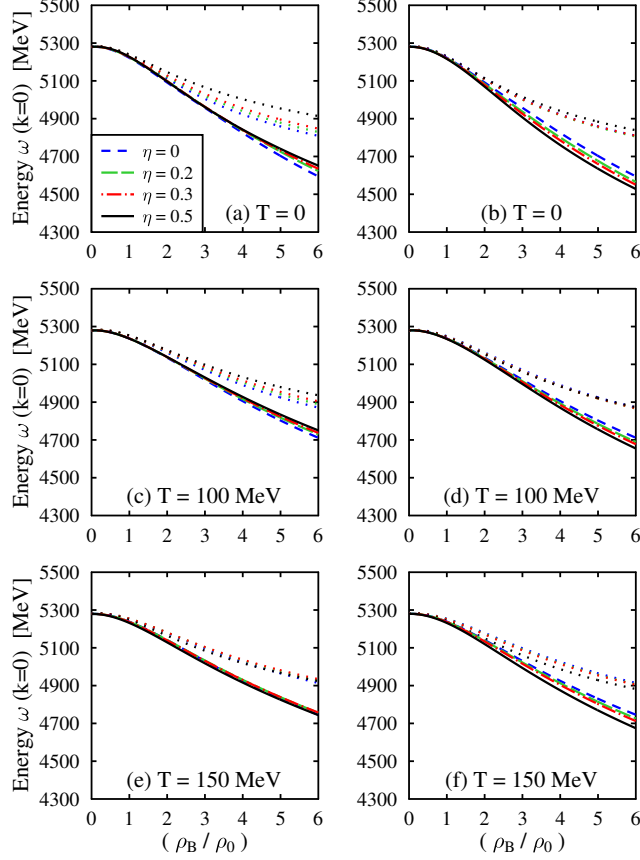


FIG. 6. (Color Online) A comparison of the energy at  $\vec{k} = 0$ , of the  $B^+$  (subplots (a), (c) and (e)) and  $B^0$  mesons (subplots (b), (d) and (f)), in hyperonic matter (with  $f_s = 0.5$ ), at various values of the isospin asymmetry parameter ( $\eta$ ), as described in the legend, and at different temperatures. In each case, this hyperonic matter situation is also compared against the nuclear matter ( $f_s = 0$ ) situation, represented by dotted lines.

respective meson, i.e.

$$U(k=0) = -\Delta m(k=0) \equiv -\Delta m(\rho_B, T, \eta, f_s), \quad (32)$$

which has been treated in detail in this article. Thus, the behavior of the intercepts follows immediately from this realization – be it the largest magnitude for  $\bar{B}^0$  between all four of these mesons, or their equivalence in the symmetric situation for the pairs  $(B^+, B^0)$  and  $(B^-, \bar{B}^0)$ , or the lower optical potentials for the  $\bar{B}$  mesons as compared to the  $B$  mesons in the symmetric situation, etc. It may additionally be noticed from the self energy expressions, given by eqns. (29) and (30), that in the symmetric situation, just like everything noted

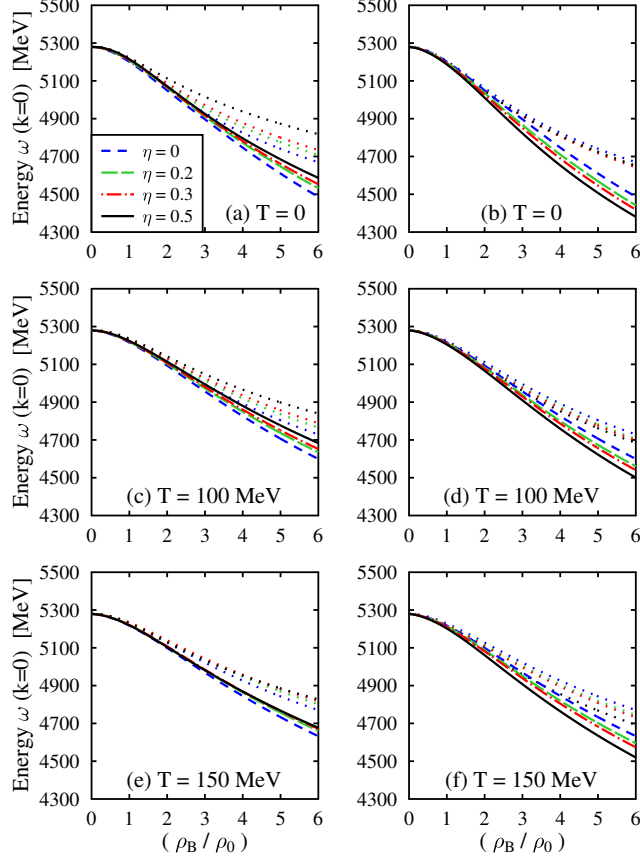


FIG. 7. (Color Online) A comparison of the energy at  $\vec{k} = 0$ , of the  $B^-$  (subplots (a), (c) and (e)) and  $\bar{B}^0$  mesons (subplots (b), (d) and (f)), in hyperonic matter (with  $f_s = 0.5$ ), at various values of the isospin asymmetry parameter ( $\eta$ ), as described in the legend, and at different temperatures. In each case, this hyperonic matter situation is also compared against the nuclear matter ( $f_s = 0$ ) situation, represented by dotted lines.

earlier, the  $k$  dependence for both the  $B$  mesons (as well as both the  $\bar{B}$  mesons) is also identical. This readily explains why the curves corresponding to  $(B^+, B^0)$  and  $(B^-, \bar{B}^0)$  mesons are identical for  $\eta = 0$ , even at finite  $k$ . In fact, the effects of non-zero strangeness, as well as non-zero asymmetry, as analyzed earlier in the  $\vec{k} = 0$  situation, extend directly to this finite momentum situation. The former is responsible for lowering the optical potentials of all four of these mesons as compared to the nuclear matter ( $f_s = 0$ ) situation, while the effect of the latter is observed to be opposite for isospin pairs, except for the somewhat anomalous behavior for the  $B^0$  meson, noted before. Also, a monotonic variation with the

isospin asymmetry parameter, as was observed with the medium masses, is reflected in the optical potentials as well. However, a general observation from the plots is that, the effect of non-zero  $k$  is to lower the optical potential from its value at zero  $k$ , which follows from the definition, eqn.(31). Both the terms,  $\omega(k)$  (calculated from the dispersion relation, with non-zero  $k$ ) and the free kinetic energy part  $(k^2 + m_B^2)^{1/2}$  are increasing functions of  $k$ . However, the former increases faster, since its  $k$  dependence arises through the factor  $k^2(1 + d_1 f_1(\rho_i^s) + d_2 f_2(\rho_i^s) - f_3(\sigma', \delta'))$  against the plain  $k^2$  of the latter. We have already discussed the behavior and interplay of these functions while studying the behavior of the total range term with density. Discounting the small density regime where the negative contribution predominates over the positive ones, the factor in parenthesis is significantly larger than 1 at larger densities, which is responsible for the observed reduction in the magnitude of optical potential with  $k$ . Also, a larger reduction with  $k$  at, e.g.  $\rho_B = 4\rho_0$ , as compared to  $\rho_B = \rho_0$ , is exactly in tow with the density dependence of this factor. Thus, with optical potentials falling monotonically with  $k$ , the largest magnitude for each of them is seen at  $k = 0$ , which is the largest for  $\bar{B}^0$  amongst all four of them, for reasons already described in detail.

Finally, we compare the results of our investigation with the existing treatments of the  $B$  and  $\bar{B}$  meson in-medium properties, using approaches other than this chiral effective model. In the quark-meson coupling approach of Ref.[15], the in-medium mass of various pseudo-scalar and vector mesons, as well as for baryons, was studied as a function of total baryonic density of the medium. The  $B$  mesons are observed to undergo, at the nuclear saturation density for example, a mass drop of about 60 MeV from its vacuum value, which is in good agreement with the 49 MeV drop that follows from our analysis. However, we notice that this approach does not distinguish between the  $B$  and  $\bar{B}$  mesons at all, which implies that it would be more sensible to compare this number against the average mass drop of  $B$  and  $\bar{B}$  mesons from our analysis, which stands at 61.5 MeV (average of 49 MeV mass drop for the  $B$  mesons and the 74 MeV drop for the  $\bar{B}$  mesons). Thus, both, the attractive nature of the interactions, as well as the magnitude of the mass drop, are in good agreement with what follows from this generalized chiral effective approach. An attractive nature of the in-medium interaction was also observed in the approach of Ref.[53], where the  $B$  meson – nucleon interaction was considered to take place exclusively through pion exchange. Here, the  $B$  mesons were found to undergo a mass drop of 106 MeV in isospin

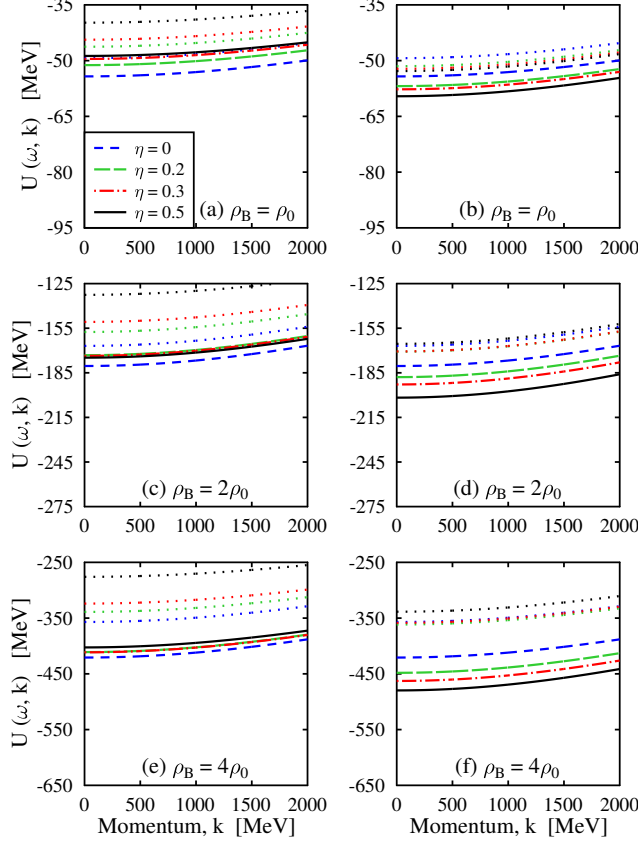


FIG. 8. (Color Online) The optical potentials of the  $B$  mesons ( $B^+$  in subplots (a), (c) and (e), and  $B^0$  in subplots (b), (d) and (f)), as a function of momentum  $k$  ( $\equiv |\vec{k}|$ ), in cold ( $T = 0$ ) hyperonic matter (with  $f_s = 0.3$ ), at various values of the isospin asymmetry parameter ( $\eta$ ), as described in the legend, and at different densities. In each case, this hyperonic matter situation is also compared against the nuclear matter ( $f_s = 0$ ) situation, represented by dotted lines.

symmetric nuclear matter, at  $\rho_B = \rho_0$ . We note however, that in this work, the authors have used  $\rho_0 = 0.17 \text{ fm}^{-3}$ , in contrast with the  $\rho_0 = 0.15 \text{ fm}^{-3}$  used in both this investigation, as well as in the QMC approach of Ref.[15]. At  $\rho_B = 0.17 \text{ fm}^{-3}$ , the value of mass drop for the  $B$  mesons in isospin symmetric nuclear matter in our work stands at 63 MeV, which is still, appreciably smaller as compared to their study. We also point out that the mass degeneracy of  $B^+$  and  $B^0$  mesons in isospin symmetric matter, and a mass splitting between these isospin pairs in the asymmetric situation, which we had observed earlier in this section, is exactly replicated in the treatment of Ref.[53]. Thus, there is a qualitative agreement between the results of these two approaches. The same authors have also adopted a different approach

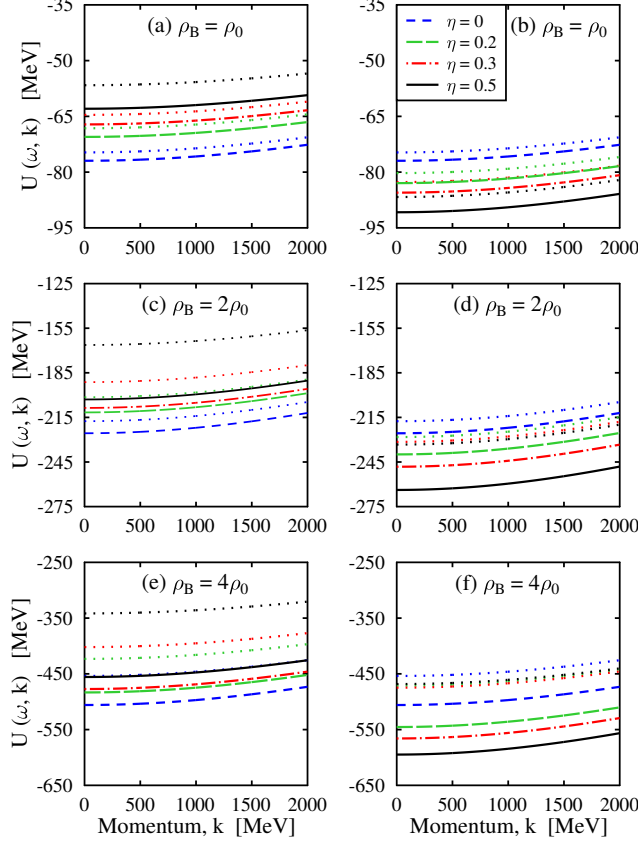


FIG. 9. (Color Online) The optical potentials of the  $\bar{B}$  mesons ( $B^-$  in subplots (a), (c) and (e), and  $\bar{B}^0$  in subplots (b), (d) and (f)), as a function of momentum  $k$  ( $\equiv |\vec{k}|$ ), in cold ( $T = 0$ ) hyperonic matter (with  $f_s = 0.3$ ), at various values of the isospin asymmetry parameter ( $\eta$ ), as described in the legend, and at different densities. In each case, this hyperonic matter situation is also compared against the nuclear matter ( $f_s = 0$ ) situation, represented by dotted lines.

towards analyzing the in-medium behavior of  $B$  mesons in Ref.[52], where these in-medium interactions have been considered from the point of view of heavy meson effective theory, with  $1/M$  corrections. This approach provides corresponding mass drops of 42 and 32 MeV corresponding to two different sets of parameter choices, at  $\rho_B = 0.17 \text{ fm}^{-3}$ , which are in even closer agreement with what we have found in this investigation, than the approach of Ref.[53]. A similar attractive nature of the  $B-N$  interaction also follows from the analysis of Ref.[78], where the  $J_P = (1/2)^- BN$  state was reported to have a binding energy of 9.4 MeV, hence implying a stable bound state. The masses of the  $B$  mesons were also observed to drop in calculations employing the QCD Sum Rules approach [11, 79]; however, an increase in

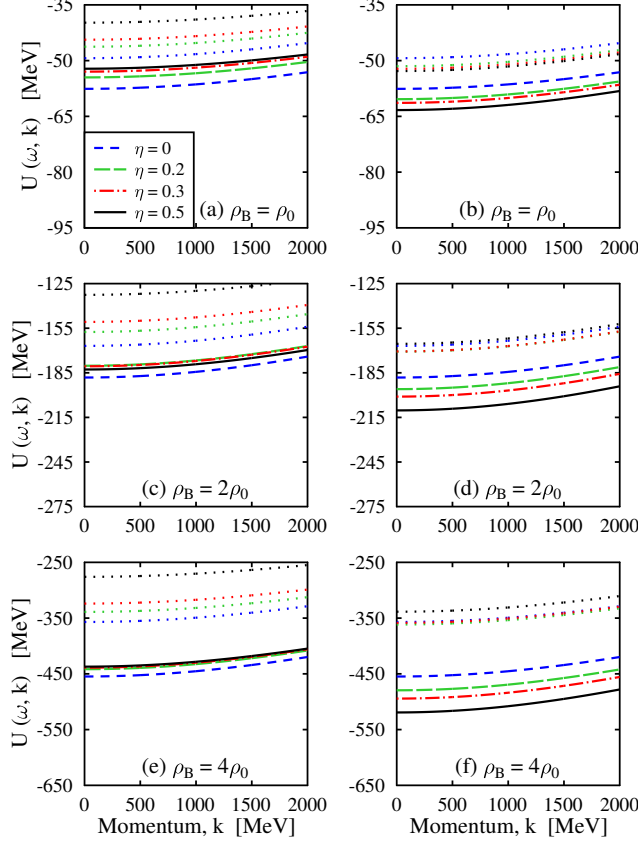


FIG. 10. (Color Online) The optical potentials of the  $B$  mesons ( $B^+$  in subplots (a), (c) and (e), and  $B^0$  in subplots (b), (d) and (f)), as a function of momentum  $k$  ( $\equiv |\vec{k}|$ ), in cold ( $T = 0$ ) hyperonic matter (with  $f_s = 0.5$ ), at various values of the isospin asymmetry parameter ( $\eta$ ), as described in the legend, and at different densities. In each case, this hyperonic matter situation is also compared against the nuclear matter ( $f_s = 0$ ) situation, represented by dotted lines.

the medium mass for the  $\bar{B}$  mesons was observed in [11], which is in contrast to the findings of this investigation. In the present work, the masses and optical potentials of the  $B$  and  $\bar{B}$  mesons in hadronic matter have been studied using an effective chiral model generalized to include the bottom sector, to derive the interactions of these mesons to the light hadrons. A systematic analysis of the effects of density and temperature, as well as sensitivity of the in-medium properties of the  $B$  and  $\bar{B}$  mesons to isospin asymmetry and strangeness fraction of the hadronic medium have been carried out in the present investigation.



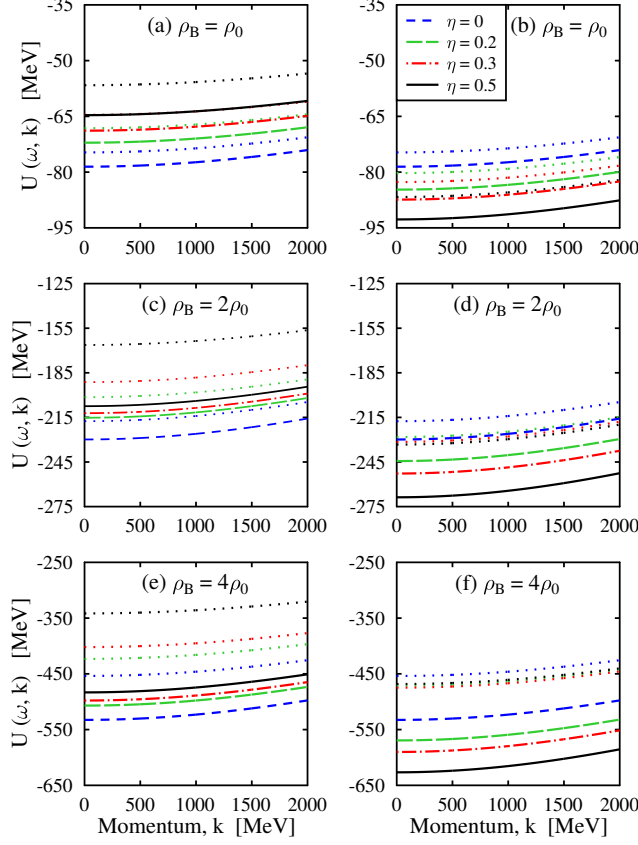


FIG. 11. (Color Online) The optical potentials of the  $\bar{B}$  mesons ( $B^-$  in subplots (a), (c) and (e), and  $\bar{B}^0$  in subplots (b), (d) and (f)), as a function of momentum  $k$  ( $\equiv |\vec{k}|$ ), in cold ( $T = 0$ ) hyperonic matter (with  $f_s = 0.5$ ), at various values of the isospin asymmetry parameter ( $\eta$ ), as described in the legend, and at different densities. In each case, this hyperonic matter situation is also compared against the nuclear matter ( $f_s = 0$ ) situation, represented by dotted lines.

## V. SUMMARY

To summarize, we have studied the in-medium masses of the  $B$  and  $\bar{B}$  mesons in hot and dense strange hadronic medium. To this end, we consider a generalization of a chiral effective model originally designed for the light quark sector. However, due to the large mass of  $b$  quark, it stays frozen in the medium, and all medium modifications are due to the light quark (or antiquark) content of these mesons. Progressively building from (isospin) symmetric cold nuclear matter to symmetric cold hyperonic matter, to include the effects of finite temperatures, to further venture into the territory of asymmetric matter, we have systemat-

ically studied the dependence of the in-medium mass of these  $B$  and  $\bar{B}$  mesons on baryonic density, temperature, strangeness and isospin asymmetry in the medium. We find that each of these mesons experiences a net attractive interaction in the medium, and possesses an in-medium mass smaller than its vacuum value at all finite densities. These medium effects are found to be strongly density dependent, with the medium mass progressively decreasing as we go to higher densities. We have restricted our discussions of the density effects on the masses  $B$  and  $\bar{B}$  mesons to about 4 times nuclear matter density. This is because, at still higher densities, the chiral effective model loses its applicability, when the hadrons are no longer the degrees of freedom, as the system undergoes a transition to quark matter. In the present investigation, we find the medium effects to be weakly temperature dependent, this weak dependence extending over the entire regime in which a hadronic phase is believed to exist (and hence, this chiral effective approach can apply). We find that the effect of addition of strangeness to the medium is to intensify the mass drops for both  $B$  and  $\bar{B}$  mesons, hence implying that the medium becomes more attractive with the addition of hyperons. The vectorial Weinberg-Tomozawa term has equal and opposite contributions for the  $B$  mesons and  $\bar{B}$  mesons, resulting in the fact that they have unequal medium masses; however, the two  $B$  mesons (as well as the two  $\bar{B}$  mesons) are degenerate in isospin symmetric matter. In an isospin asymmetric medium, however, even this degeneracy gets broken, and all four of these mesons possess unequal masses, with the  $\bar{B}^0$  meson experiencing the largest amount of mass drop in the medium. Also, for all of them, this dependence on density, asymmetry and strangeness is also reflected in their in-medium optical potentials. Each of these observed features finds a requisite explanation from the point of view their self energies in the medium, derived from their interaction Lagrangian density in this chiral effective model. The in-medium behavior we find on the basis of this generalization of this chiral effective model, bodes well with independent calculations based on alternative methods, wherever such a comparison is possible. To the best of our knowledge, the effect of strangeness and temperature on the in-medium properties of  $B$  and  $\bar{B}$  mesons, as well as an analysis of the in-medium behavior of these mesons at densities larger than the normal matter density ( $\rho_0$ ), are all features hitherto unconsidered in the literature.

## ACKNOWLEDGMENTS

A.M. would like to thank Department of Science and Technology, Government of India (Project No. SR/S2/HEP-031/2010) for financial support. D.P. acknowledges financial support from University Grants Commission, India [Sr. No. 2121051124, Ref. No. 19-12/2010(i)EU-IV].

- 
- [1] C. M. Ko, V. Koch and G. Q. Li, *Annu. Rev. Nucl. Part. Sci.* **47**, 505 (1997).
  - [2] R. S. Hayano and T. Hatsuda, *Rev. Mod. Phys.* **80**, 2949 (2010).
  - [3] G. Q. Li, *Prog. Part. Nucl. Phys.* **43**, 619 (1999).
  - [4] N. K. Glendenning, *Compact Stars – Nuclear Physics, Particle Physics and General Relativity*, 2<sup>nd</sup> edition. (Springer, 2000).
  - [5] J. A. Oller, E. Oset and J. R. Peláez, *Phys. Rev. Lett.* **80**, 3452 (1998).
  - [6] E. Oset and A. Ramos, *Nucl. Phys. A* **635**, 99 (1998).
  - [7] L. Tolós, J. Schaffner-Bielich and A. Mishra, *Phys. Rev. C* **70**, 025203 (2004).
  - [8] J. Hofmann and M. F. M. Lutz, *Nucl. Phys. A* **763**, 90 (2005).
  - [9] M. A. Shifman, A. I. Vainshtein and V. I. Zakharov, *Nucl. Phys. B* **147**, 448 (1979).
  - [10] A. Hayashigaki, *Phys. Lett. B* **487**, 96 (2000).
  - [11] T. Hilger, R. Thomas and B. Kämpfer, *Phys. Rev. C* **79**, 025202 (2009).
  - [12] A. Kumar and A. Mishra, *Phys. Rev. C* **82**, 045207 (2010).
  - [13] K. Tsushima, D. H. Lu, A. W. Thomas, K. Saito and R. H. Landau, *Phys. Rev. C* **59**, 2824 (1999).
  - [14] A. Sibirtsev, K. Tsushima and A. W. Thomas, *Eur. Phys. J. A* **6**, 351 (1999).
  - [15] K. Tsushima and F. C. Khanna, *Phys. Lett. B* **552**, 138 (2003).
  - [16] B. D. Serot and J. D. Walecka, *Int. J. Mod. Phys. E* **6**, 515 (1997).
  - [17] D. B. Kaplan and A. E. Nelson, *Phys. Lett. B* **175**, 57 (1986).
  - [18] G. Q. Li, C. M. Ko and G. E. Brown, *Phys. Rev. Lett.* **75**, 4007 (1995).
  - [19] G. Q. Li and C. M. Ko, *Nucl. Phys. A* **582**, 731 (1995).
  - [20] G. Q. Li, C. M. Ko and G. E. Brown, *Nucl. Phys. A* **606**, 568 (1996).
  - [21] A. Sibirtsev, K. Tsushima, K. Saito and A. W. Thomas, *Phys. Lett. B* **484**, 23 (2000).

- [22] Q. Li, Z. Li, S. Soff, M. Bleicher and H. Stöcker, J. Phys. G **32**, 407 (2006).
- [23] A. Andronic, P. Braun-Munzinger, K. Redlich and J. Stachel, Phys. Lett. B **659**, 149 (2008).
- [24] P. Papazoglou, D. Zschesche, S. Schramm, J. Schaffner-Bielich, H. Stöcker and W. Greiner, Phys. Rev. C **59**, 411 (1999).
- [25] D. Zschesche et al., ‘*Chiral Symmetries in Nuclear Physics*’, in *Symmetries in Intermediate and High Energy Physics*, Springer Tracts in Modern Physics, Vol. 163 (Springer-Verlag, 2000).
- [26] D. Zschesche, A. Mishra, S. Schramm, H. Stöcker and W. Greiner, Phys. Rev. C **70**, 045202 (2004).
- [27] A. Mishra, K. Balazs, D. Zschesche, S. Schramm, H. Stöcker and W. Greiner, Phys. Rev. C **69**, 024903 (2004).
- [28] A. Mishra, E. L. Bratkovskaya, J. Schaffner-Bielich, S. Schramm and H. Stöcker, Phys. Rev. C **70**, 044904 (2004).
- [29] A. Mishra and S. Schramm, Phys. Rev. C **74**, 064904 (2006).
- [30] A. Mishra, S. Schramm and W. Greiner, Phys. Rev. C **78**, 024901 (2008).
- [31] A. Mishra, A. Kumar, S. Sanyal and S. Schramm, Eur. Phys. J. A **41**, 205 (2009).
- [32] A. Mishra, A. Kumar, S. Sanyal, V. Dexheimer and S. Schramm, Eur. Phys. J. A **45**, 169 (2010).
- [33] A. Mishra, E. L. Bratkovskaya, J. Schaffner-Bielich, S. Schramm and H. Stöcker, Phys. Rev. C **69**, 015202 (2004).
- [34] A. Mishra and A. Mazumdar, Phys. Rev. C **79**, 024908 (2009).
- [35] A. Kumar and A. Mishra, Phys. Rev. C **81**, 065204 (2010).
- [36] A. Kumar and A. Mishra, Eur. Phys. J. A **47**, 164 (2011).
- [37] S. H. Lee and C. M. Ko, Phys. Rev. C **67**, 038202 (2003).
- [38] S. H. Lee and C. M. Ko, Prog. Theor. Phys. Suppl. **149**, 173 (2003).
- [39] A. Mishra and D. Pathak, Phys. Rev. C **90**, 025201 (2014).
- [40] J. M. Torres-Rincon, L. Tolos and O. Romanets, Phys. Rev. D **89**, 074042 (2014).
- [41] G. D. Moore and D. Teaney, Phys. Rev. C **71**, 064904 (2005).
- [42] M. He, R. J. Fries and R. Rapp, Phys. Rev. C **86**, 014903 (2012).
- [43] L. M. Abreu, D. Cabrera and J. M. Torres-Rincon, Phys. Rev. D **87**, 034019 (2013).
- [44] S. K. Das, S. Ghosh, S. Sarkar and J. Alam, Phys. Rev. D **85**, 074017 (2012).
- [45] M. He, R. J. Fries and R. Rapp, Phys. Lett. B **735**, 445 (2014).

- [46] BaBar Collaboration, Official Webpage, <http://www-public.slac.stanford.edu/babar>
- [47] BELLE Collaboration, Official Webpage, <http://belle.kek.jp>
- [48] J. Brodzicka et al. (BELLE Collaboration), Prog. Theor. Exp. Phys. 04D001 (2012).
- [49] BELLE-II Collaboration, Official Webpage, <http://belle2.kek.jp>
- [50] BELLE-II experiment, Official Website of DESY, <http://belle2.desy.de>
- [51] BELLE-II Technical Design Report, KEK Report 2010-1, arXiv:1011.0352 [physics.ins-det]
- [52] S. Yasui and K. Sudoh, Phys. Rev. C **89**, 015201 (2014).
- [53] S. Yasui and K. Sudoh, Phys. Rev. C **87**, 015202 (2013).
- [54] S. Yasui and K. Sudoh, Phys. Rev. C **88**, 015201 (2013).
- [55] S. Weinberg, Phys. Rev. Lett. **18**, 188 (1967).
- [56] S. Weinberg, Phys. Rev. **166**, 1568 (1968).
- [57] S. Coleman, J. Wess and B. Zumino, Phys. Rev. **177**, 2239 (1969).
- [58] C. G. Callan, S. Coleman, J. Wess and B. Zumino, Phys. Rev. **177**, 2247 (1969).
- [59] W. A. Bardeen and B. W. Lee, Phys. Rev. **177**, 2389 (1969).
- [60] G. E. Brown and M. Rho, Phys. Rev. Lett. **66**, 2720 (1991).
- [61] E. K. Heide, S. Rudaz, P. J. Ellis, Nucl. Phys. A **571**, 713 (2001).
- [62] J. Schechter, Phys. Rev. D **21** 3393 (1980).
- [63] F. Klingl, S. Kim, S. H. Lee, P. Morath, and W. Weise, Phys. Rev. Lett. **82**, 3396 (1999).
- [64] J. Beringer et al. (Particle Data Group), Phys. Rev. D **86**, 010001 (2012), and 2013 partial update for the 2014 edition.
- [65] A. Bazavov et al. (Fermilab Lattice and MILC Collaboration), Phys. Rev. D **85**, 114506 (2012).
- [66] H. Na et al. (HPQCD Collaboration), Phys. Rev. D **86**, 034506 (2012).
- [67] S. Narison, Phys. Lett. B **718**, 1321 (2013).
- [68] S. Narison, Phys. Lett. B **721**, 269 (2013).
- [69] P. Gelhausen, A. Khodjamirian, A. A. Pivovarov and D. Rosenthal, Phys. Rev. D **88**, 014015 (2013).
- [70] M. J. Baker et al. (ETM Collaboration), JHEP07, 032 (2014).
- [71] W. Lucha, D. Melikhov, and S. Simula, J. Phys. G **38**, 105002 (2011).
- [72] R. J. Dowdall, C. T. H. Davies, R. R. Horgan, C. J. Monahan, and J. Shigemitsu (HPQCD Collaboration), Phys. Rev. Lett. **110**, 222003 (2013).

- [73] D. Röder, J. Ruppert and D. H. Rischke, Phys. Rev. D **68**, 016003 (2003).
- [74] Y. Aoki, G. Endrődi, Z. Fodor, S. D. Katz and K. K. Szabó, Nature **443**, 675 (2006).
- [75] C. Bernard et al. (MILC Collaboration), Phys. Rev. D **71**, 034504 (2005).
- [76] A. Bazavov et al. (HotQCD Collaboration), Phys. Rev. D **85**, 054503 (2012).; A. Bazavov et al., Phys. Rev. Lett. **113**, 072001 (2014).
- [77] W. Weise - “*Quarks, Hadrons and Dense Nuclear Matter*”, lectures in proceedings of Trends in Nuclear Physics, 100 years later, Les Houches, Session LXVI, 1996.
- [78] S. Yasui and K. Sudoh, Phys. Rev. D **80**, 034008 (2009).
- [79] K. Azizi, N. Er and H. Sundu, arXiv:1405.3058 [hep-ph]